

## Green Strategies for Design and Construction of Non-Auto Transportation Infrastructure

Maryam Nazari

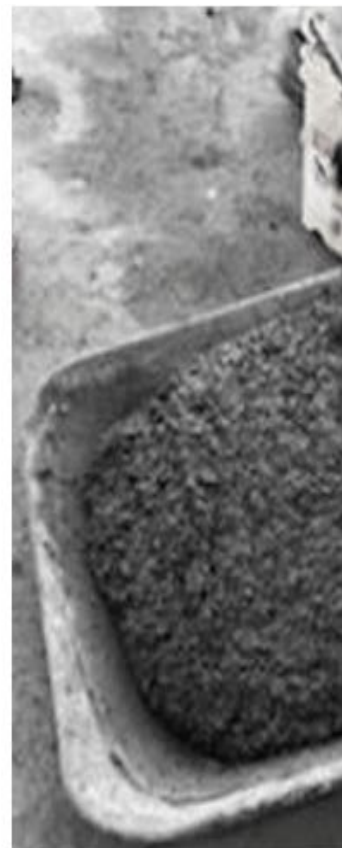
Fariborz Tehrani

Mojtaba Ansari

Bhavesh Jeevanlal

Faiaz Rahman

Roshanak Farshidpour



# MINETA TRANSPORTATION INSTITUTE

Founded in 1991, the Mineta Transportation Institute (MTI), an organized research and training unit in partnership with the Lucas College and Graduate School of Business at San José State University (SJSU), increases mobility for all by improving the safety, efficiency, accessibility, and convenience of our nation's transportation system. Through research, education, workforce development, and technology transfer, we help create a connected world. MTI leads the four-university MTI leads the four-university California State University Transportation Consortium funded by the State of California through Senate Bill 1.

MTI's transportation policy work is centered on three primary responsibilities:

## Research

MTI works to provide policy-oriented research for all levels of government and the private sector to foster the development of optimum surface transportation systems. Research areas include: bicycle and pedestrian issues; financing public and private sector transportation improvements; intermodal connectivity and integration; safety and security of transportation systems; sustainability of transportation systems; transportation / land use / environment; and transportation planning and policy development. Certified Research Associates conduct the research. Certification requires an advanced degree, generally a Ph.D., a record of academic publications, and professional references. Research projects culminate in a peer-reviewed publication, available on TransWeb, the MTI website (<http://transweb.sjsu.edu>).

## Education

The Institute supports education programs for students seeking a career in the development and operation of surface transportation systems. MTI, through San José State University, offers an AACSB-accredited Master of Science in Transportation Management and graduate certificates in Transportation Management, Transportation Security, and High-Speed Rail Management that serve to prepare the nation's transportation managers for the 21st century. With the

active assistance of the California Department of Transportation (Caltrans), MTI delivers its classes over a state-of-the-art videoconference network throughout the state of California and via webcasting beyond, allowing working transportation professionals to pursue an advanced degree regardless of their location. To meet the needs of employers seeking a diverse workforce, MTI's education program promotes enrollment to under-represented groups.

## Information and Technology Transfer

MTI utilizes a diverse array of dissemination methods and media to ensure research results reach those responsible for managing change. These methods include publication, seminars, workshops, websites, social media, webinars, and other technology transfer mechanisms. Additionally, MTI promotes the availability of completed research to professional organizations and journals and works to integrate the research findings into the graduate education program. MTI's extensive collection of transportation-related publications is integrated into San José State University's world-class Martin Luther King, Jr. Library.

---

## Disclaimer

The contents of this report reflect the views of the authors, who are responsible for the facts and accuracy of the information presented herein. This document is disseminated in the interest of information exchange. The report is funded, partially or entirely, by a grant from the State of California. This report does not necessarily reflect the official views or policies of the State of California or the Mineta Transportation Institute, who assume no liability for the contents or use thereof. This report does not constitute a standard specification, design standard, or regulation.

REPORT 19-17

# GREEN STRATEGIES FOR DESIGN AND CONSTRUCTION OF NON-AUTO TRANSPORTATION INFRASTRUCTURE

Maryam Nazari,  
Fariborz Tehrani,  
Mojtaba Ansari,  
Bhavesh Jeevanlal,  
Faiaz Rahman,  
Roshanak Farshidpour

July 2019

A publication of

**Mineta Transportation Institute**

Created by Congress in 1991

College of Business  
San José State University  
San José, CA 95192-0219

# TECHNICAL REPORT DOCUMENTATION PAGE

<b>1. Report No.</b> 19-17	<b>2. Government Accession No.</b>	<b>3. Recipient's Catalog No.</b>	
<b>4. Title and Subtitle</b> Green Strategies for Design and Construction of Non-Auto Transportation Infrastructure		<b>5. Report Date</b> July 2019	
		<b>6. Performing Organization Code</b>	
<b>7. Authors</b> Maryam Nazari, <a href="https://orcid.org/0000-0002-5170-943">https://orcid.org/0000-0002-5170-943</a> Fariborz Tehrani Mojtaba Ansari Bhavesh Jeevanlal Faiaz Rahman Roshanak Farshidpour		<b>8. Performing Organization Report</b> MTI Report CA-MTI-1872	
<b>9. Performing Organization Name and Address</b> Mineta Transportation Institute College of Business San José State University San José, CA 95192-0219		<b>10. Work Unit No.</b>	
		<b>11. Contract or Grant No.</b> ZSB12017-SJAUX	
<b>12. Sponsoring Agency Name and Address</b> State of California SB1 2017/2018 Trustees of the California State University Sponsored Programs Administration 401 Golden Shore, 5th Floor Long Beach, CA 90802		<b>13. Type of Report and Period Covered</b> Final Report	
		<b>14. Sponsoring Agency Code</b>	
<b>15. Supplemental Notes</b>			
<b>16. Abstract</b> Application of Tire-Derived Aggregates (TDA) as a green, durable, and economically-efficient material, enhances the sustainability of transportation infrastructure. Throughout the course of this research study, the application of TDA in combination with expanded clay (EC) aggregates will be investigated in concrete slabs used in road pavements and bridge decks serving non-auto traffic, such as bicycle routes, through a set of experimental tests and life-cycle cost analyses. To this end, TDA, which is obtained from recycled tires, and EC, produced in rotary kilns, substitute coarse aggregates in conventional concrete. The final product, also known as lightweight rubberized concrete, is durable and economically-efficient. It also enhances the sustainability of transportation infrastructure by mitigating the necessary maintenance and rehabilitation needs of these slabs. In this report, an experimental study has been undertaken to first estimate mechanical properties of lightweight rubberized concrete using 100% EC, 100% TDA, and a mixture of 20% EC – 80% TDA; the TDA was replaced by the volume of the EC aggregates. Next, a series of static flexural and dynamic impact-fatigue tests were performed on simply-supported beam specimens and slab assemblies, respectively, to measure both modulus of rupture and durability when subjected to the applied loads. The cyclic testing results confirmed a lower flexural strength of the rubberized concrete specimens. However, the specimens exhibited an ability to withstand larger plastic deformations up until the point of failure. Using the results of impact-fatigue tests, a life-cycle cost analysis was also performed, which confirmed long-term benefits of constructing green and durable infrastructure, using TDA and EC, on transportation investments. In conclusion, using these durable materials in infrastructural construction will lessen their maintenance and rehabilitation needs. Further, this application will divert waste tires from landfills.			
<b>17. Key Words</b> Sustainability, bicycle routes, rubberized concrete pavements, expanded clay, life cycle analysis	<b>18. Distribution Statement</b> No restrictions. This document is available to the public through The National Technical Information Service, Springfield, VA 22161		
<b>19. Security Classif. (of this report)</b> Unclassified	<b>20. Security Classif. (of this page)</b> Unclassified	<b>21. No. of Pages</b> 42	<b>22. Price</b>

Copyright © 2019  
by **Mineta Transportation Institute**  
All rights reserved

Mineta Transportation Institute  
College of Business  
San José State University  
San José, CA 95192-0219

Tel: (408) 924-7560  
Fax: (408) 924-7565  
Email: [mineta-institute@sjsu.edu](mailto:mineta-institute@sjsu.edu)

[transweb.sjsu.edu](http://transweb.sjsu.edu)

## **ACKNOWLEDGMENTS**

This study was supported by both the CSU Transportation Consortium and the Fresno State Transportation Institute. Any opinions, findings, conclusions, and recommendations expressed in this material are those of the authors and do not necessarily reflect the views of these institutes. We greatly appreciate the laboratory personnel of Fresno State, Steve Scherer, Arthur Hauzer, and Derick Gangbin for their assistance in conducting the experimental research presented in this report. A sincere thank you is also extended to graduate and undergraduate students of Fresno State, Zeinab Younis, Nathanael Torres, Francisco Perez, Eduardo Bravo, and Armando Cervantes for their assistance in fabricating the test units. Donation of materials by Trinity Lightweight is also greatly appreciated.

The authors thank Editing Press, for editorial services, as well as MTI staff, including Executive Director Karen Philbrick, PhD; Deputy Executive Director Hilary Nixon, PhD; Graphic Designer Alverina Eka Weinardy; and Executive Administrative Assistant Jill Carter.

---

## TABLE OF CONTENTS

<b>Executive Summary</b>	<b>1</b>
<b>I. Introduction and Objectives</b>	<b>2</b>
<b>II. Literature Review</b>	<b>4</b>
Tire-Derived Aggregate Concrete	4
Expanded Clay	6
<b>III. Experimental Program</b>	<b>7</b>
Design Mixes and Materials	7
Description of Test Specimens	8
Fabrication and Assembly of Test Specimens	9
Test Setup, Loading Protocol, and Instrumentation	12
<b>IV. Experimental Results and Discussion</b>	<b>19</b>
Phase I: Materials Testing	19
Phase II: Part 1 – Static Flexural Tests of Beams	22
Phase II: Part 2 – Impact Fatigue Tests of Slabs	26
<b>V. Life-Cycle Cost Analysis</b>	<b>29</b>
Initial Costs	29
Maintenance Costs	29
<b>VI. Conclusions and Future Research</b>	<b>32</b>
<b>Abbreviations and Acronyms</b>	<b>34</b>
<b>Endnotes</b>	<b>35</b>
<b>Bibliography</b>	<b>38</b>
<b>About the Authors</b>	<b>41</b>

---

## LIST OF FIGURES

1. Tire-Derived Aggregate Concrete	3
2. Sieve Analysis Results of Expanded Clay Aggregates	7
3. Dowel Bar Connection in Slab Assemblies	9
4. Construction of Specimens	11
5. Universal Testing Machine (UTM) for Materials Testing	12
6. Overview of Experimental Setup and Instrumentation for Beams	14
7. Loading Protocol – Beam Testing	15
8. Overview of Experimental Setup and Instrumentation for Slabs	16
9. Modeling of Slab Assemblies in SAP2000	17
10. Tensile Stress Distribution at the Bottom Face of the Slabs with MIX A when Subjected to Impact Loading, $P_{max}$	18
11. Fracture Pattern According to ASTM C39	19
12. Fracture Pattern in Cylindrical Specimens – Compression Test	21
13. Average Compressive Strength of Concrete Cylinders	22
14. Experimental Observations – Static Flexural Testing of Beams	23
15. Stress-Strain Curves for Beams with MIX A, B, and C	25
16. Flexural Toughness vs Rubber Content in Beams	26
17. Number of Loading Cycles vs. Strain – Impact Fatigue Testing of Slab Assemblies	27
18. Initial Cost of Materials Per Cubic Meter of Concrete	29
19. Schematic Relationship Between Stress and Load Cycles	30

---

## LIST OF TABLES

1. Design Mix for 1 ft <sup>3</sup> of Concrete – Control Mix (MIX A)	8
2. Design Mix Proportion in ft <sup>3</sup> for 1 ft <sup>3</sup> of Concrete	8
3. Design Mix Proportion in lb for 1 ft <sup>3</sup> of Concrete	8
4. Test Matrix (for Each Concrete Mix)	8
5. Compressive Strength of Cylinders – MIX A	19
6. Compressive Strength of Cylinders – MIX B	20
7. Compressive Strength of Cylinders – MIX C	20
8. Summary of Experimental Results – Beams	25
9. Summary of Experimental Results	30
10. Summary of Cost Analyses	31

## EXECUTIVE SUMMARY

The application of Tire-Derived Aggregates (TDA) as a green, durable, and economically-efficient material, enhances the sustainability of transportation infrastructure. Throughout the course of this research study, the application of TDA in combination with expanded clay (EC) aggregates will be investigated in concrete slabs used in road pavements and bridge decks serving non-auto traffic, such as bicycle routes, through a set of experimental tests and life-cycle cost analyses. To this end, TDA, which is obtained from recycled tires, and EC, produced in rotary kilns, substitute coarse aggregates in conventional concrete. The final product, also known as lightweight rubberized concrete, is durable and economically-efficient. It also enhances the sustainability of transportation infrastructure by mitigating the necessary maintenance and rehabilitation needs of these slabs. In this report, an experimental study has been undertaken to first estimate mechanical properties of lightweight rubberized concrete using 100% EC, 100% TDA, and a mixture of 20% EC – 80% TDA; the TDA was replaced by the volume of the EC aggregates. Next, a series of static flexural and dynamic impact-fatigue tests were performed on simply-supported beam specimens and slab assemblies, respectively, to measure both modulus of rupture and durability when subjected to the applied loads. The cyclic testing results confirmed a lower flexural strength of the rubberized concrete specimens. However, the specimens exhibited an ability to withstand larger plastic deformations up until the point of failure. Using the results of impact-fatigue tests, a life-cycle cost analysis was also performed, which confirmed long-term benefits of constructing green and durable infrastructure, using TDA and EC, on transportation investments. In conclusion, using these durable materials in infrastructural construction will lessen their maintenance and rehabilitation needs. Further, this application will divert waste tires from landfills.

---

## I. INTRODUCTION AND OBJECTIVES

Non-auto transportation infrastructure serves as an efficient and environmentally conscious means for public mobility. An initiative towards sustainable design and construction of the concrete slabs that compose these routes promotes both green sources of materials and reduced economic maintenance costs over their life cycle. As a result, this research aims to investigate the application of tire-derived aggregates (TDA) in combination with expanded clay (EC) aggregates in precast concrete slabs in road pavements and bridge decks serving non-auto traffic, such as bicycle routes. Given that TDA is a recycled, durable, and economically-efficient material, this project aims to enhance its usage and its ability to increase the sustainability of such transportation infrastructure, along with attempting to influence future decision-making on the rehabilitation and maintenance of such roads.

The use of precast concrete elements in pavement applications has been successfully applied for over 40 years in the United States. Precast concrete has also proven to be a durable, high-performance solution for bridges. Based on this precedence of reliability, precast concrete panels will be used for pavement and bridge deck applications to design and construct the non-auto transportation routes in this project.

Incorporated within this research, TDA, which is recycled from waste rubber materials in tires, replaces coarse aggregates in concrete, to address the long-term maintenance and rehabilitation needs of the precast concrete slabs (see Figure 1). Tires are made of durably engineered materials in order to provide safe, reliable, and predictable behavior for wheels of vehicles. As a result, using these materials will facilitate the construction of infrastructure with similar beneficial properties, reducing their maintenance and rehabilitation needs while also mitigating the amount of waste tires sitting in landfills. In this project, EC was also used as an efficient and durable lightweight coarse aggregate suitable for a wide range of applications in construction. The application of EC in precast concrete slabs allows the easy movement and transportation of these members. The final product, namely lightweight rubberized concrete has higher energy dissipation when compared to conventional concrete. This enhancement of energy absorption places TDA concrete at a unique advantage over its conventional counterpart. This, however, comes at a cost, as rubberized concrete has a lower strength than conventional, and as a result, an optimal balance must be reached between energy absorption and strength.<sup>1-3</sup>

This research project explores the possibility of applying TDA concrete in precast concrete slabs and bridge decks through the investigation of their mechanical properties and overall performance for non-auto transportation applications. Furthermore, a life-cycle cost analysis will be conducted to investigate the long-term benefits of constructing green and durable infrastructure on future investments in transportation.



**Figure 1. Tire-Derived Aggregate Concrete**

---

## II. LITERATURE REVIEW

An extensive review of literature related to material properties of TDA and EC was undertaken as part of this study and is summarized in the following sections. Results from prior experimental findings on sustainable concrete components and structures using these materials are also highlighted herein.

### TIRE-DERIVED AGGREGATE CONCRETE

According to the California Department of Resources Recycling and Recovery (CalRecycle), the state currently generates approximately 40 million waste tires per year. As a result, CalRecycle urges researchers to work towards finding the advantages of the recycled material. TDA has already been used for several applications in California, including embankment fill material, retaining wall backfill material, vibration damping material, asphalt pavements, and traffic barriers.<sup>4</sup> Several research studies have been performed to increase the diversion of waste tires from landfills by promoting TDA in Civil Engineering applications, as presented below.

Several researchers have conducted research in reference to the hardened properties of concrete.<sup>5-7</sup> They provided analysis pertaining to the difference in the content of tire aggregates within concrete, and the ultimate impact on the compressive and splitting tensile strength. It was concluded that although these hardened properties of concrete decreased with an increase in rubber content, the material still contained a large energy absorption capacity. The reduction in compressive strength as discussed in prior studies has been traced to being caused by entrapped air. As a result, some experiments increased the compressive strength of the rubberized concrete by simply by incorporating de-airing agents within the mix.<sup>8</sup>

Rostami et al.<sup>9</sup> provided further analysis with regard to proper bonding between rubber particles and cement paste when incorporating tire aggregates with a rough surface or pretreatment within the concrete mix, resulting in a higher compressive strength. The paper concluded that concrete containing water-washed rubber particles has a larger compressive strength by approximately 16%.

Segre and Joekes<sup>10</sup> presented work on the surface modification of tire rubber, ultimately increasing the adhesion of rubber to cement. The rubber aggregate used within the experiment was treated on the surface with NaOH for a time span of 20 minutes, prior to mixing with other materials. A comparison of the results from (a) as-received tire aggregate concrete mix and (b) NaOH-treated tire aggregate concrete mix concluded that the latter has a higher toughness and results in a reduction in porosity.

In a study conducted by Siddique and Naik<sup>11</sup>, the physical properties of concrete containing scrap-tire rubber were obtained. The paper discussed how the application of shredded/chipped tires, as well as ground rubber, affects the concrete's properties when compared to crumb rubber aggregates. Conducting the slump test allowed these researchers to determine the workability of fresh concrete through the use of assorted tire aggregate (i.e., shredded/chipped and crumb) at 10%, 20%, 40%, 60%, 80%, and 100% rubber

replacements by the volume of the coarse aggregate. With an increase in rubber content within the mixture, it was concluded that there was a decrease in slump values. Additional properties discussed throughout the course of the experiment included air content and unit weight of the rubberized concrete. Considering the dependence of unit weight on air content within a mixture, the research showed that an increase in the rubber content increases the air content, thereby decreasing the unit weight of concrete.

Al-Tayeb et al.<sup>2</sup> analyzed the performance of rubberized and hybrid concrete structures under static and impact load conditions. Throughout the course of their experiment, rubberized concrete samples were developed (with the dimensions of 1.97-inch x 3.94-inch x 5.91-inch) with 5%, 10%, and 20% replacement of sand (fine aggregate) by waste crumb rubber. Three types of specimens were used within the experiment, including plain concrete, rubberized concrete, and double layer concrete (with rubberized concrete placed on the upper region and plain concrete on the bottom). In addition to a conventional hammer impact test, all of the specimens were statically tested under a three-point bending load in accordance with ASTM C78.<sup>12</sup> It was shown that partial substitution of fine aggregate by rubber, reduced compressive and tensile stresses by 5–20% and 11–17%, respectively. The elastic modulus determined was also found to be reduced by 8–22%. Plotting the obtained bending loads against displacement for each specimen showed that the bending loads increased with an increase in the percentage of sand replacement by crumb rubber. Maximum bending loads were observed in the hybrid specimen. Furthermore, the rubberized portion at the upper region of the hybrid specimen, subject to impact loads, had enhanced the specimen's ability to absorb energy.

Vadivel<sup>13</sup> created a total of 12 cylindrical specimens (150-mm diameter and 64-mm height) categorized into 4 groups.  $R_0$  was established as the control specimen used within the experiment;  $R_1$  contained 6% rubber crumbs replacement by the volume of the fine aggregate (FA);  $R_2$  contained 6% rubber crumbs replacement by the volume of the coarse aggregate (CA);  $R_3$  contained 3% rubber crumbs and 3% chiseled truck tire chip replacements for FA and CA. When conducting the experiment, impact testing was performed using the equipment fabricated within the laboratory, which contained a standard manual operated 7.72-lb compaction hammer with a 48-inch drop. The hammer was dropped repeatedly, and the number of blows required to form both the first visible crack within the upper surface of the specimen as well as at ultimate failure was recorded. It was shown that  $R_1$  was able to consume approximately 80% of the input energy due to impacts. These samples failed through gradual compression.  $R_2$  consumed the least energy when placed in comparison with the other specimens.  $R_3$  showed significant plastic energy and withstood large deformations, which indicated a larger energy dissipation capacity of the specimen.

Miller and Tehrani<sup>14</sup> provided further research regarding the toughness and ductility of lightweight rubberized concrete for rubber replacement ratios of 0% to 100% at 20% increments for lightweight expanded shale aggregates. It was concluded that the strength of concrete mixtures is reduced with the addition of rubber particles. Within the experiment, a dynamic impact flexure test on a concrete beam sized 6-inch x 6-inch x 21-inch was also performed in order to determine the toughness index and ductility of the rubberized concrete through a falling mechanism. To perform the test, a falling weight was dropped

from a height determined using a simplified energy equation. This equation relates to the minimum strength and corresponding deflection observed during a static flexure test. The dynamic results were obtained through recording the acceleration–time history of test units using an accelerometer. This allowed the force-time relationship and net impulse for each drop to be calculated. It was also observed that the value of flexural strength decreased nonlinearly as the rubber replacement ratios varied from 0% to 100%. However, flexural toughness and energy dissipation capacity of the concrete significantly increased at rubber replacement values of 80% and 100%.

## **EXPANDED CLAY**

Lightweight Expanded Clay (EC) aggregates have a long history of incorporation in structures dating to ancient civilizations, but their structural properties have been studied in more depth as their usage has increased in the past 70 years.<sup>15</sup> Initially, lightweight aggregates in general were made from volcanic rock material, such as pumice and tuff, but increasing demand has forced the industrial development of such aggregates.<sup>16</sup> EC is specifically composed of materials including shale, clay, and slate, and is produced within rotary kilns at 1100°C.<sup>17</sup> The resulting expandability of EC makes it a reliable, durable, and lightweight material. Mainly used for cast-in-place skyscrapers and bridge decks, EC is now frequently employed in precast applications, where its lightweight nature allows the easy handling and transportation of precast concrete members without compromising their structural integrity.<sup>18</sup>

To the authors' knowledge, no published data is available on the application of both TDA and EC in concrete pavement slabs, serving non-auto traffic. To this end, this project aims to investigate the durability and sustainability of these concrete elements through a set of impact fatigue testing, which mainly replicates the loading condition caused by bicycles, as well as life-cycle cost analyses.

### III. EXPERIMENTAL PROGRAM

This research study investigates the acceptability of lightweight rubberized concrete application in non-auto transportation slabs using a series of experimental tests. The experimental program is composed of two phases: materials testing (Phase I) and structural components testing (Phase II). The latter consists of two parts: static flexural testing of beam specimens (Phase II- Part 1) and dynamic impact-fatigue testing of slab assemblies (Phase II- Part 2). In what follows, a detailed description of the test units, experimental setups, and instrumentations is presented.

#### DESIGN MIXES AND MATERIALS

Lee et al.<sup>19</sup> studied the mechanical properties of the roller-compacted concrete used in biking pavements. In accordance with their research, a concrete compressive strength of 3000 psi would be appropriate for the biking loading, which has also been used in this research study. To evaluate the mechanical properties of rubberized lightweight aggregate concrete, Miller and Tehrani<sup>14</sup> also incorporated a 3000 psi compressive strength for the control mix.

Three mix designs were considered in this research, including 0% (MIX A), 80% (MIX B), and 100% (MIX C) TDA replacements by the volume of the light-weight EC coarse aggregates. The mix containing 0% replacement ratio was used as the control mix. The rubber replacement ratios of 80% and 100% were selected following the recommendations of Miller and Tehrani<sup>14</sup> to achieve a higher flexural toughness for the specimens. The unit weight of TDA and EC is respectively 71.8 and 107.9 pcf with the corresponding specific gravity of 1.15 and 1.73. Note that the size of TDA is 3/8-inch and it does not contain any steel fibers. Figure 2 presents the sieve analysis results of EC aggregates.

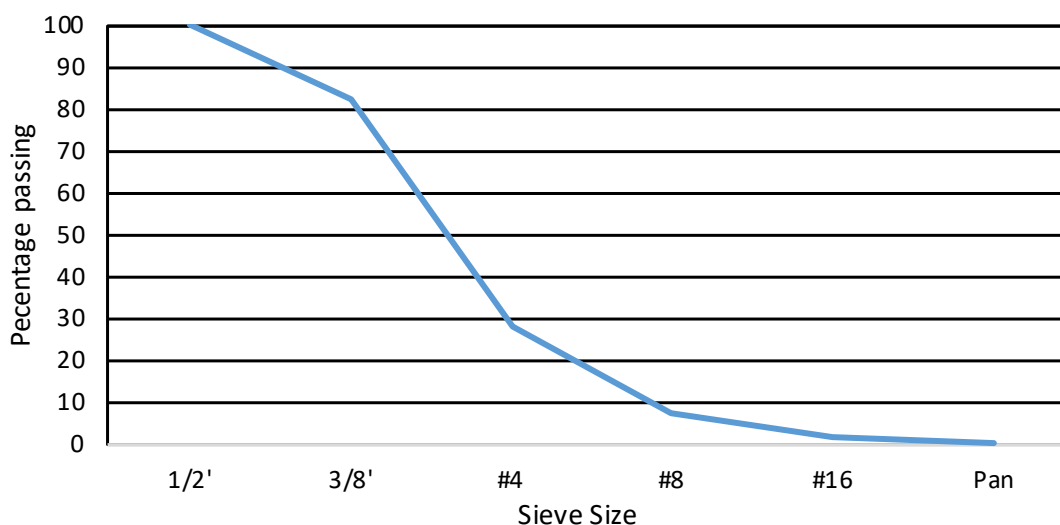


**Figure 2. Sieve Analysis Results of Expanded Clay Aggregates**

Table 1 shows the concrete mix design calculation for one ft<sup>3</sup> volume of MIX A. Tables 2 and 3 respectively present the volume and weight of the materials required to cast one ft<sup>3</sup> of concrete. The total weight/volume of the materials was calculated by estimating the volume of all test specimens used in this research (i.e., cylinders, beams, and slabs).

**Table 1. Design Mix for 1 ft<sup>3</sup> of Concrete – Control Mix (MIX A)**

Material	Desired proportion by weight	Specific gravity	lb per 100 lb of cement	Volume (ft <sup>3</sup> )	
A	B	C	D	E	F
			$D = B \times 100$	$E = D / (62.4 C)$	$F = E / \text{Total Volume}$
Cement	1.00	3.15	100	0.509	0.168
Water	0.48	1	48	0.769	0.255
Fine Aggregate	1.52	2.65	151.8	0.918	0.304
LWA	0.89	1.73	89.1	0.825	0.273
	Sum		<b>388.95</b>	<b>3.022</b>	<b>1.000</b>

**Table 2. Design Mix Proportion in ft<sup>3</sup> for 1 ft<sup>3</sup> of Concrete**

MIX	Water	Cement	Sand, FA	LWA	TDA	Total
A – Control	0.255	0.168	0.304	0.273	0.000	1.0
B – 80%	0.255	0.168	0.304	0.055	0.219	1.0
C – 100%	0.255	0.168	0.304	0.000	0.273	1.0

**Table 3. Design Mix Proportion in lb for 1 ft<sup>3</sup> of Concrete**

MIX	Water	Cement	Sand, FA	LWA	TDA	Total
A	15.88	33.09	50.25	29.49	0.00	128.7
B	15.88	33.09	50.25	5.90	15.68	120.8
C	15.88	33.09	50.25	0.00	19.60	118.8

## DESCRIPTION OF TEST SPECIMENS

Table 4 summarizes the test matrix. The information provided in this table reflects the number of specimens for each concrete mix.

**Table 4. Test Matrix (for Each Concrete Mix)\***

Specimen	Size	Number	Test
Phase I – Cylinder	6 in. (diameter) × 12 in. (height) (ASTM Standard) <sup>20</sup>	3	Compression Testing
Phase II – Part 1 Beam	21 in. (length) × 6 in. (width) × 6 in. (height) (ASTM Standard) <sup>12</sup>	3	Static Flexural Testing
Phase II – Part 2 Slab	27 in. (length) × 18 in. (width) × 4 in. (thickness)	1	Impact-Fatigue Testing

\* Three different concrete mix designs (MIX A-C) are used in this research study.

The original dimensions of the slabs were 42-inch  $\times$  42-inch  $\times$  4-inch, joined along the longitudinal direction using conventional dowel bar connections with the transverse spacing of 18-inch. For the purpose of testing, the slab width was considered to be equal to the spacing of the bars, so that the test unit only accommodated for one set of connectors. Furthermore, a length of 27-inch was considered for each slab to ensure that the two wheels of the bicycle, with an average wheelbase (i.e., the distance between the front and rear axles of a bicycle) of 18-inch, were positioned on each slab. These test specimens were properly constrained in the experimental setup to reflect the actual condition of the slabs.

### Design of the Dowel Bars in Slabs

The dowel bars, with 18-inch spacing, were designed for the shear forces acting near the joint. The diameter of the dowel bar was calculated using the shear strength of the material and the applied shear force at the connection. Consequently, one No. 3 bar with a total length of 12.5-inch (with a 0.5-inch gap between the slabs) was used to join the slabs, as shown in Figure 3. Also, following ACI 318-14<sup>18</sup>, a minimum temperature and shrinkage reinforcement was designed for the slabs. To this end, two layers of  $\frac{1}{2}$ -inch 19 gauge galvanized welded wire mesh with the dimensions of 24-inch  $\times$  15-inch was placed in each slab, with a cover concrete of 1.5-inch.

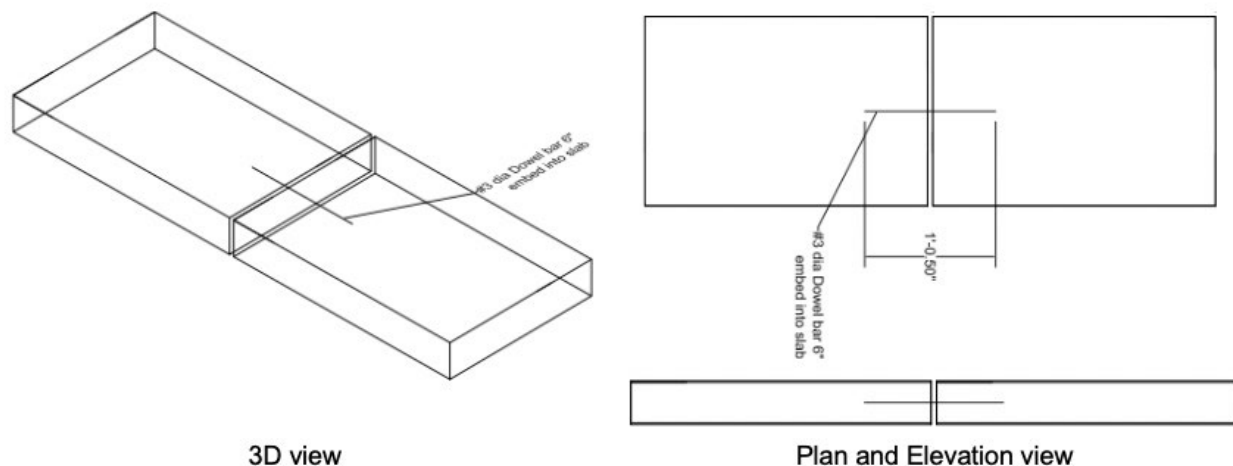


**Figure 3. Dowel Bar Connection in Slab Assemblies**

### FABRICATION AND ASSEMBLY OF TEST SPECIMENS

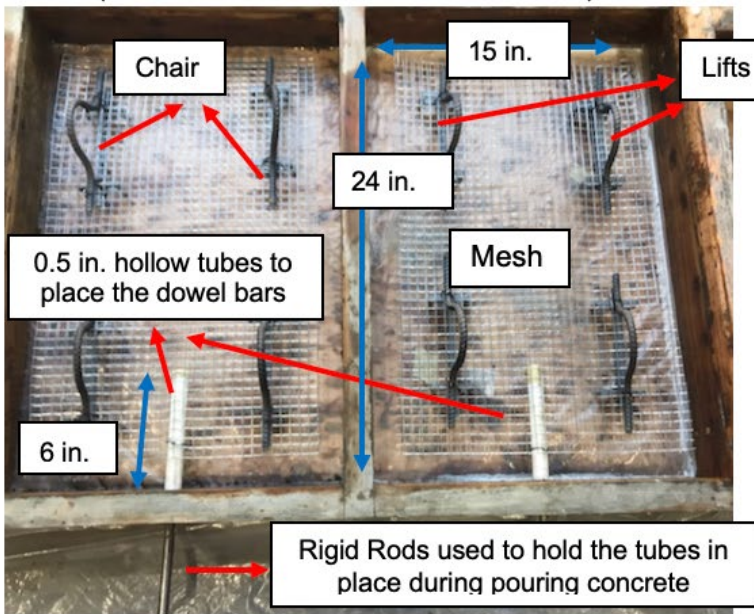
Figure 4 shows the construction of the concrete specimens and their placement in the curing room. Throughout the course of experimentation, a set of smart sensors, using electroactive materials, were used in one of the beams: MIX C (see Figure 4). The data collected by these sensors was compared to that of those captured using physical sensors and was presented in the proceedings of IMAC XXXVII – Society for Experimental Mechanics (SEM) Conference.<sup>20</sup>



Fabricated timber mold  
(reused for three different concrete mixes)



Height of the plastic chairs used  
to hold the mesh in the mold



Mold before pouring concrete



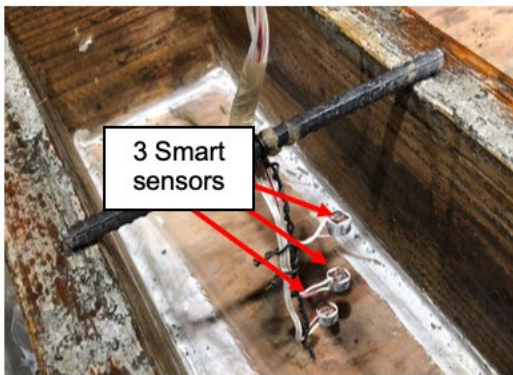
Welded wire mesh



Slump Test (an average slump of 6–7 in. was reported for different mixes)



Fabricated concrete specimens



Placement of smart sensors in the beam



Beam specimens in the curing room

**Figure 4. Construction of Specimens**

## TEST SETUP, LOADING PROTOCOL, AND INSTRUMENTATION

### Phase I: Materials Testing

The compressive strength of the concrete was measured by breaking cylindrical concrete specimens, after 28 days of curing, in a compression testing machine. ASTM C39 standard<sup>20</sup> test method for Compressive Strength of Cylindrical Concrete Specimens was followed for the testing of the specimens. The Universal Testing Machine (UTM) located within the concrete laboratory at Fresno State was used for the testing of specimens (see Figure 5).



**Figure 5. Universal Testing Machine (UTM) for Materials Testing**

In this test, a compressive axial load was applied to the smooth surface of the cylindrical specimen, and specimens containing an uneven or rough surface were sawed or ground to ensure accurate results were obtained. The loading rate in accordance with the ASTM standard is 900 lb/sec, which was maintained throughout the course of testing. Loading was continued until compressive failure of the specimens was reached. Compressive strength was then calculated by dividing the failure load by the cross-sectional area of the cylinders.

---

## **Phase II: Part 1 – Structural Components Testing: Beams**

This phase presents static flexural testing of simply-supported concrete beams. As shown in Figure 6, supports were placed 1.5-inch from each end of the beam and bearing pads were placed in between the supports and each beam itself in order to prevent stress concentrations at these locations. The experimental setup for four-point flexural testing of beams consisted of a vertical load cell with a built-in string pot (SPOT), to measure vertical displacement, and a triangular load applicator to distribute the region of maximum stress across the middle 6-inch portion of the beams (see Figure 6). The speed of the loading was set to ensure that a static loading of the beams was maintained. As shown in Figure 6, at the mid-span, two 60-mm strain gauges were placed at the top and bottom surfaces of the beams, along with a vertical linear variable deformation transducer (LVDT) to measure the maximum vertical deflections. The LVDT was mounted on a fixed support on the frame of the loading apparatus, allowing it to connect with the beam for measurements. The LVDT and SPOT were connected to a DataPAC data acquisition system for recording, while the strain gauges were connected to a separate data acquisition system. The sampling rate of both data acquisition systems were 500 ms and these two data sources were later synchronized with one another prior to data analysis.

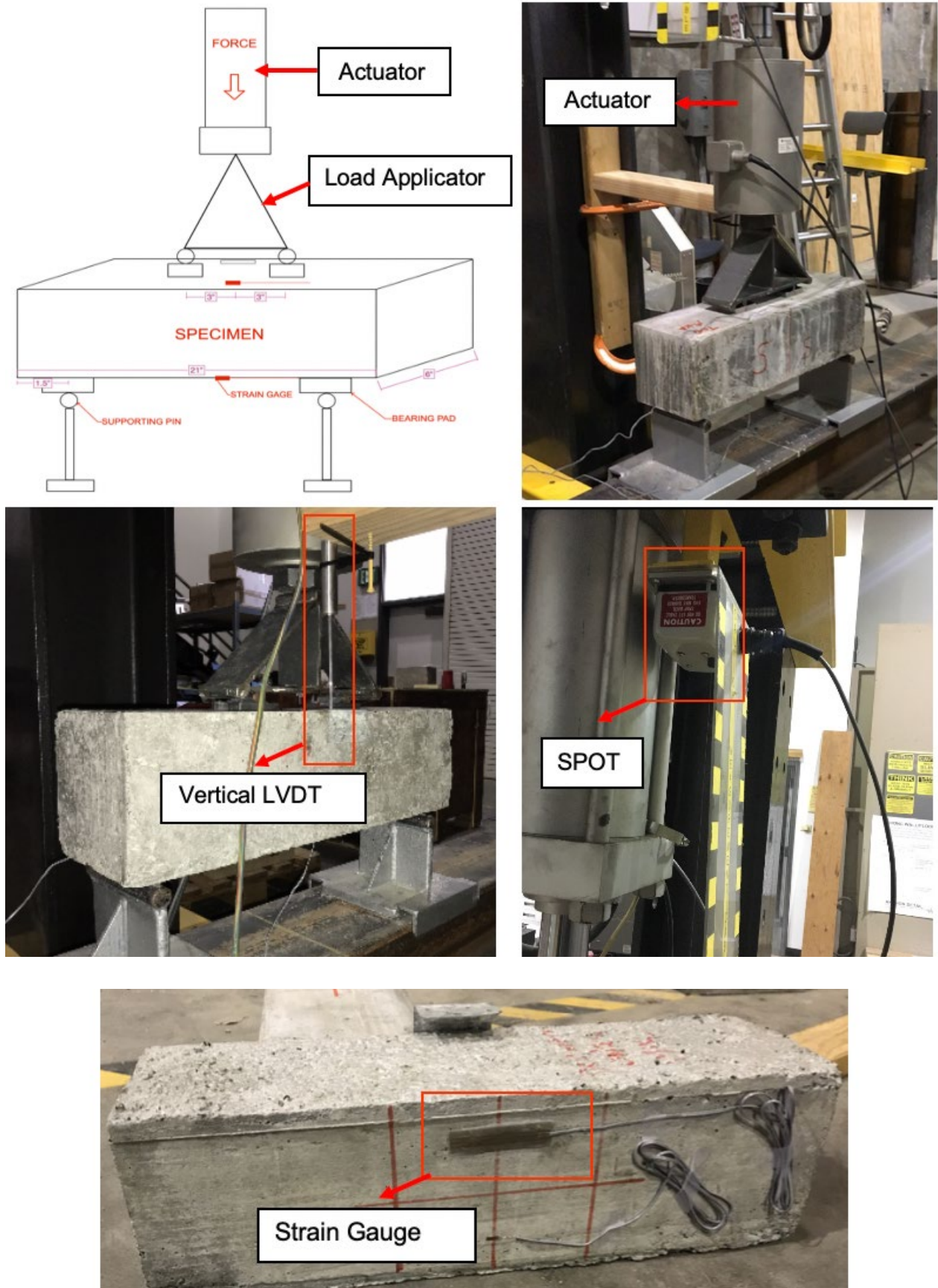
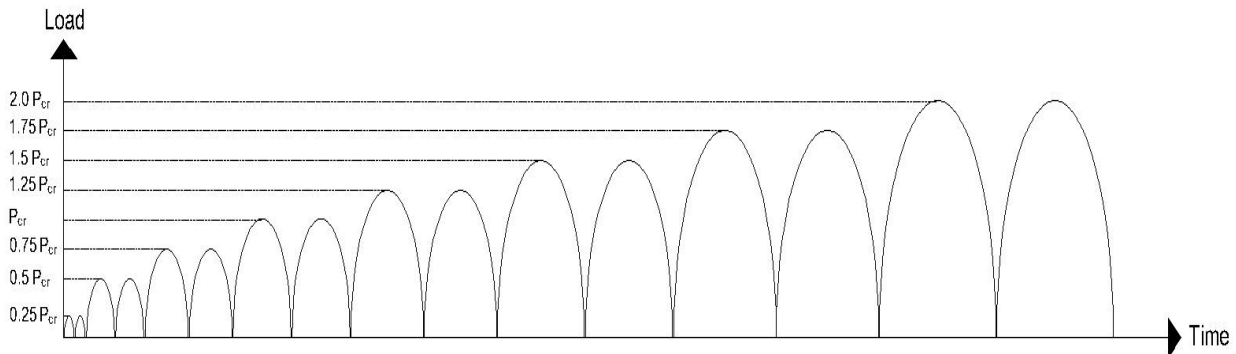


Figure 6. Overview of Experimental Setup and Instrumentation for Beams

For this research, half-cyclic flexural testing of beams was conducted to mimic biking load condition on the concrete specimens (i.e., push-release). ACI 437<sup>22</sup> testing protocol was used for the tests. The cyclic load test consisted of the application of loads in increments until the point of failure. Using ACI 318 guidelines, the modulus of rupture was calculated for each beam. Using these values, the equivalent failure stress was computed and used to estimate the critical load value  $P_{cr}$ , which would then be used to determine the load increments. The load increments were as follows:  $0.25P_{cr}$ ,  $0.50P_{cr}$ ,  $0.75P_{cr}$ ,  $P_{cr}$ ,  $1.25P_{cr}$ ,  $1.50P_{cr}$ , and  $2.00P_{cr}$  (see Figure 7). As shown in Figure 7, two cycles were applied at each load increment. It was noted that the beam specimens had the possibility of breaking before their entire loading sequence was completed.



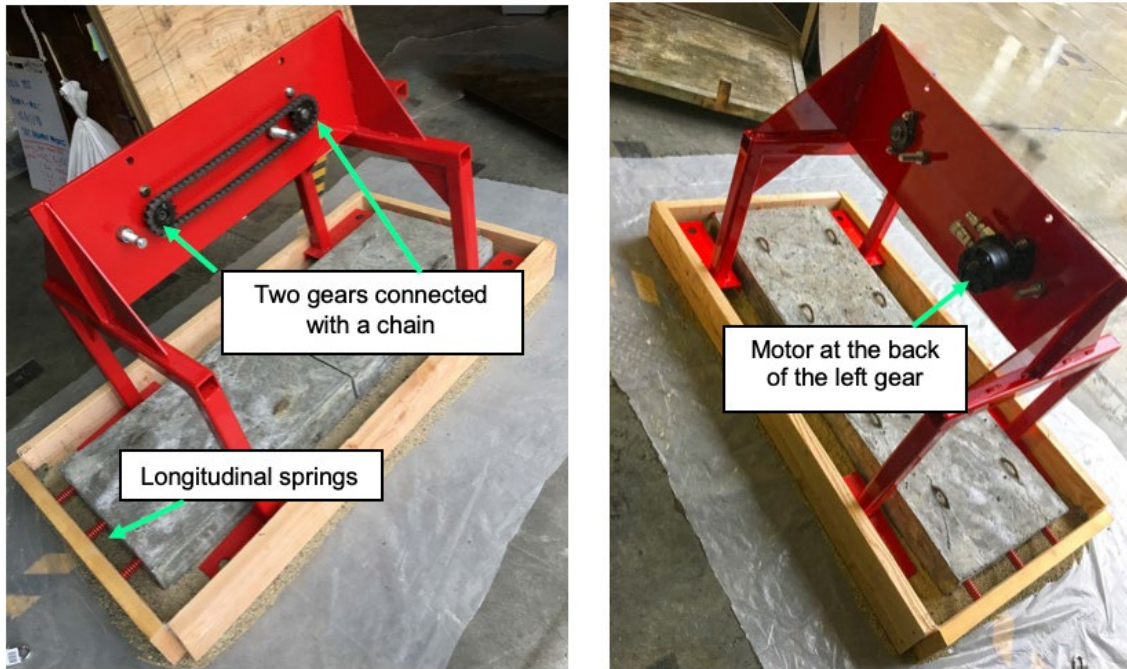
**Figure 7. Loading Protocol – Beam Testing**

## **Phase II: Part 2 – Structural Components Testing: Slabs**

Impact-fatigue testing was performed on slab assemblies to evaluate their service-life performance when subjected to several impact loads caused by bicycles. This test was performed using the equipment fabricated within the structural lab of Fresno State, as shown in Figure 8. In this setup, the impact force was produced by dropping a weight from a certain height (following the basic principles of free fall and impact in mechanics) and the fatigue feature was added by using a motor, set with a certain frequency, to repeat the impact cycles. As shown in Figure 8, two gears were attached to the structural frame. These gears were then connected with each other using a chain, while one of these gears was additionally connected to the motor at its back. Two 18-lb weights, spaced at a wheelbase distance of 18-inch, were attached to the gears. Note that a 1-inch slot was fabricated in the gears that allowed for the free fall of the weights while the gears were rotating.

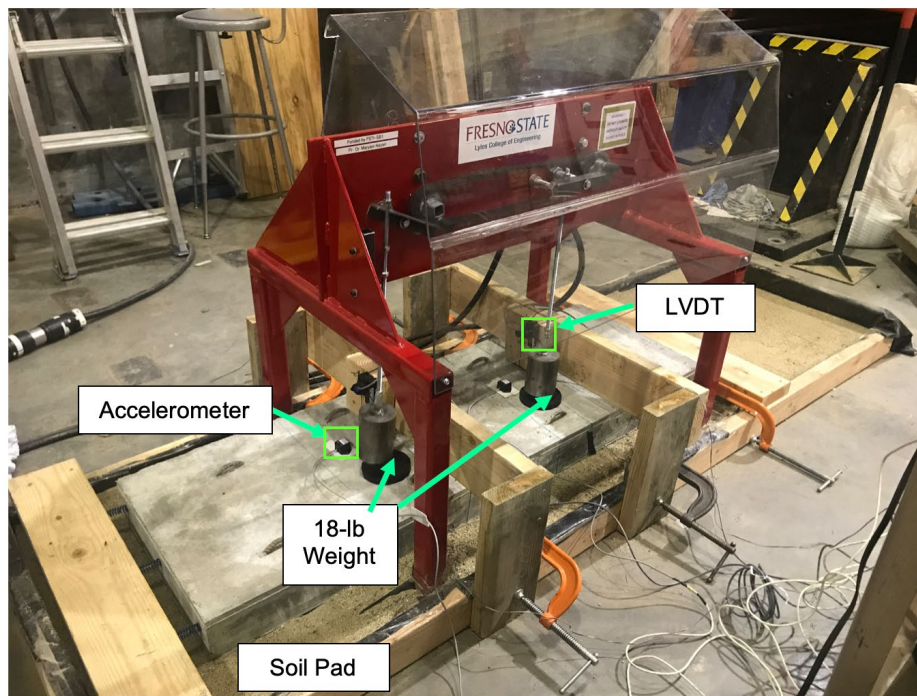
The slabs were placed inside a soil box to be supported by the soil pad (see Figure 8) and constrained in the longitudinal direction using a series of springs at their outer ends. The stiffness of these springs was estimated to accommodate for a horizontal movement of the slabs due to temperature change (i.e., equal to the spacing between the slabs). The slabs were connected with each other using a No. 3 dowel bar at their interior surface.

A series of sensors were attached to the slabs to measure their responses. This included 90-mm strain gauges at the bottom (tension) surface of the slabs, two SPOTs to measure deflections at the location of the impact load, and two accelerometers.



Front View

Back View



Completed Setup

**Figure 8. Overview of Experimental Setup and Instrumentation for Slabs**

### Impact Loading on Concrete Slabs – Analytical Modeling

An analytical study was performed using SAP2000<sup>23</sup> to estimate the maximum tensile stresses developed in the slabs due to impacts. The SAP model is presented in Figure 9. As shown in this figure, the soil pad, placed beneath the concrete slabs, was modeled with a series of springs, with the stiffness calculated using the following equation (FEMA 356<sup>24</sup>). This equation is used for slabs that are flexible comparing to the supporting soil.

$$k_{sv} = \frac{1.3G}{B(1 - \nu)} \quad (1)$$

where  $G$  is the shear modulus,  $B$  is the width of slab, and  $\nu$  is the Poisson's ratio. The theoretical value of  $K_{sv}$ , as calculated using Equation 1, was then experimentally verified by applying a constant static load on the slabs and measuring the corresponding displacements by SPOT. This verification was conducted through a trial and error process and by changing the compaction ratio of sand.

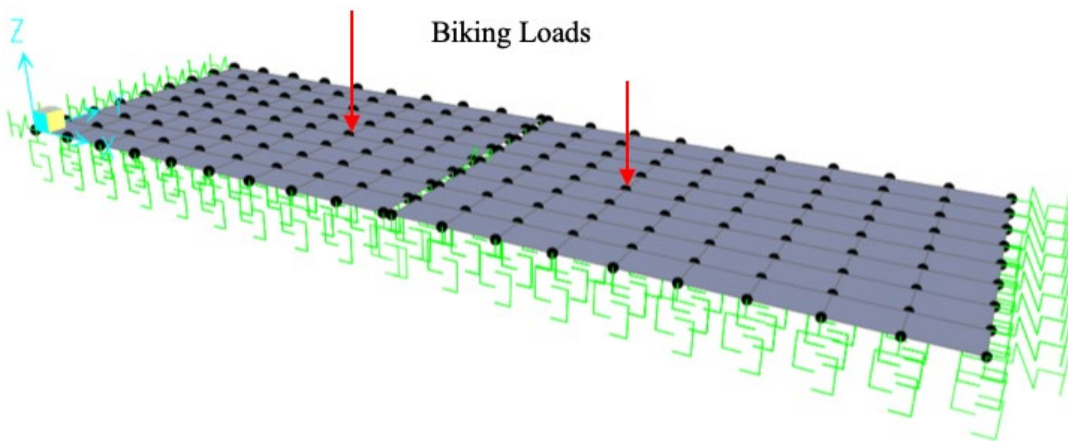


**Figure 9. Modeling of Slab Assemblies in SAP2000**

In this model, the slabs were allowed to move freely in the transverse direction but were partially restricted in the longitudinal direction with “line springs”. These springs simulated the friction caused by the adjacent slabs and their stiffness was computed using  $f = k\Delta$ , where  $f$  is the friction force acting on adjacent slab,  $\Delta$  is the max distance that slabs are allowed to move longitudinally (i.e., 0.25-inch), and  $k$  is the stiffness of the representative spring. The friction force acting beneath each slab was calculated using  $f = \mu N$ , where  $\mu = \tan \phi$  is the friction coefficient between the precast concrete and soil (sand),  $\phi$  is the friction angle of sand (in this study 30°), and  $N$  is the vertical load acting on adjacent slabs (in this case, the weight of the slabs). Accordingly, a friction force of 69.7 lb was estimated, which resulted in a stiffness of 358.3 lb/in. for the “line springs”. The two slabs were also connected at their interior surfaces, using a “link spring” to allow for free horizontal movement relative to one another.

Equation 2 was used to estimate the impact force,  $P_{max}$ , exerted on the slabs due to the falling weights,  $P_{st}$ , of 18 lb from a height  $h$  of 1-inch.

$$P_{max} = nP_{st} = \left( 1 + \sqrt{1 + 2 \left( \frac{h}{\Delta_{st}} \right)} \right) P_{st} \quad (2)$$

Using the SAP2000 model, a static deformation,  $\Delta_{st}$ , of 3.33, 3.85, and 4.26-10<sup>-4</sup> inch, was recorded at the location of point loads for MIX A, B and C, respectively, which resulted in the corresponding theoretical impact forces of 4.43, 4.12, and 3.92 kips (using Equation 2). When the slabs were loaded with these equivalent impact forces, a maximum tensile stress of 186 (MIX A), 173 (MIX B) and 165 psi (MIX C) was estimated, as shown in Figure 10 for MIX A. These values are 36%, 67% and 81% of the corresponding tensile strength values, as recorded for the beams and reported in Table 8.

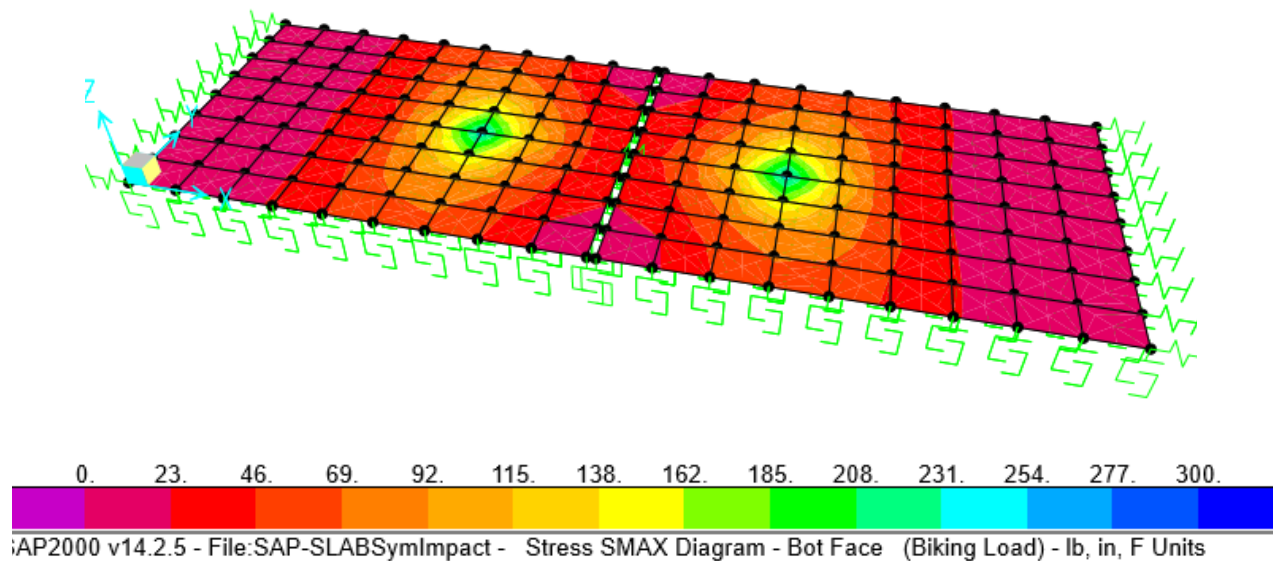


**Figure 10. Tensile Stress Distribution at the Bottom Face of the Slabs with MIX A when Subjected to Impact Loading,  $P_{max}$**

## IV. EXPERIMENTAL RESULTS AND DISCUSSION

### PHASE I: MATERIALS TESTING

After the cylinders were removed from the curing room, they were placed in the UTM and loaded until a large drop in loading was observed or the specimen experienced some fracture pattern. Once the specimen cracked, the loading was stopped, and the final load and type of fracture pattern were recorded. The recorded load was divided by the area of the specimen to determine the compressive strength of the concrete. Five types of typical fracture patterns are shown in Figure 11, following ASTM C39.<sup>20</sup>

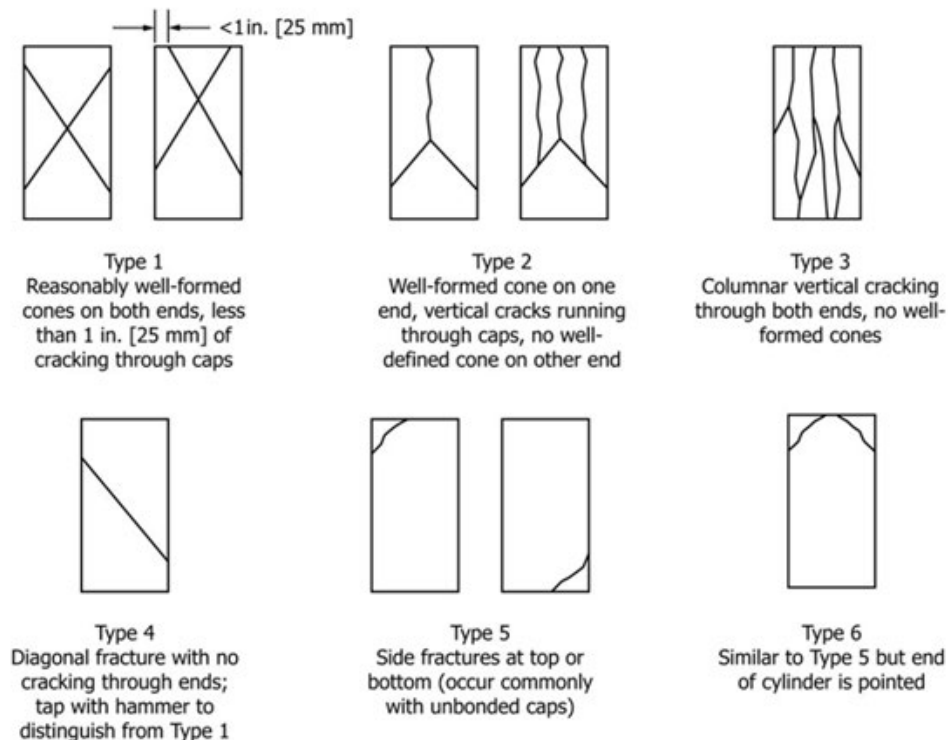


FIG. 2 Schematic of Typical Fracture Patterns

### Figure 11. Fracture Pattern According to ASTM C39<sup>20</sup>

Tables 5 to 7 and Figure 12 present information about the compressive testing of a total of 9 cylinders (three per mix design).

**Table 5. Compressive Strength of Cylinders – MIX A**

Trial number	Area of specimen (in <sup>2</sup> )	Maximum loading (lb.)	Compressive strength (psi)	Fracture Pattern
1	28.28	70,810	2504	III
2	28.28	94,050	3326	III
3	28.28	71,060	2513	III
4*	28.28	89,700	3718	III

\* One additional batch was tested for the control mix (MIX A).

**Table 6. Compressive Strength of Cylinders – MIX B**

Trial number	Area of specimen (in <sup>2</sup> )	Maximum loading (lb.)	Compressive strength (psi)	Fracture pattern
1	28.28	28,080	993	V/VI
2	28.28	23,990	848	V/VI
3	28.28	25,020	885	V/VI

**Table 7. Compressive Strength of Cylinders – MIX C**

Trial number	Area of specimen (in <sup>2</sup> )	Maximum loading (lb.)	Compressive strength (psi)	Fracture pattern
1	28.28	18,390	651	V/VI
2	28.28	13,190	446	V/VI
3	28.28	13,150	465	V/VI



**Figure 12. Fracture Pattern in Cylindrical Specimens – Compression Test**

As shown in Figure 13, the average concrete strength of MIX A, B, and C are 3015, 909, and 521 psi, respectively. Given that the design compressive strength of concrete was 3000 psi, it can be stated that 30% and 17% of the desired compressive strength were achieved, respectively, for MIX B and C, due to the replacement of coarse aggregates with tire-derived aggregates. It is important to note that this strength is sufficient in sustaining bicycle loads in non-auto transportation routes. Also, as shown in Figure 12, only localized cracks were observed at corners of the rubberized concrete cylinders while one single

crack split the control specimen (with MIX A) into two pieces. It can be concluded that a more consistent and ductile type of fracture was observed in the concrete cylinders with added rubber aggregates compared to the control specimen, which fractured in a brittle manner with little warning prior to complete failure.

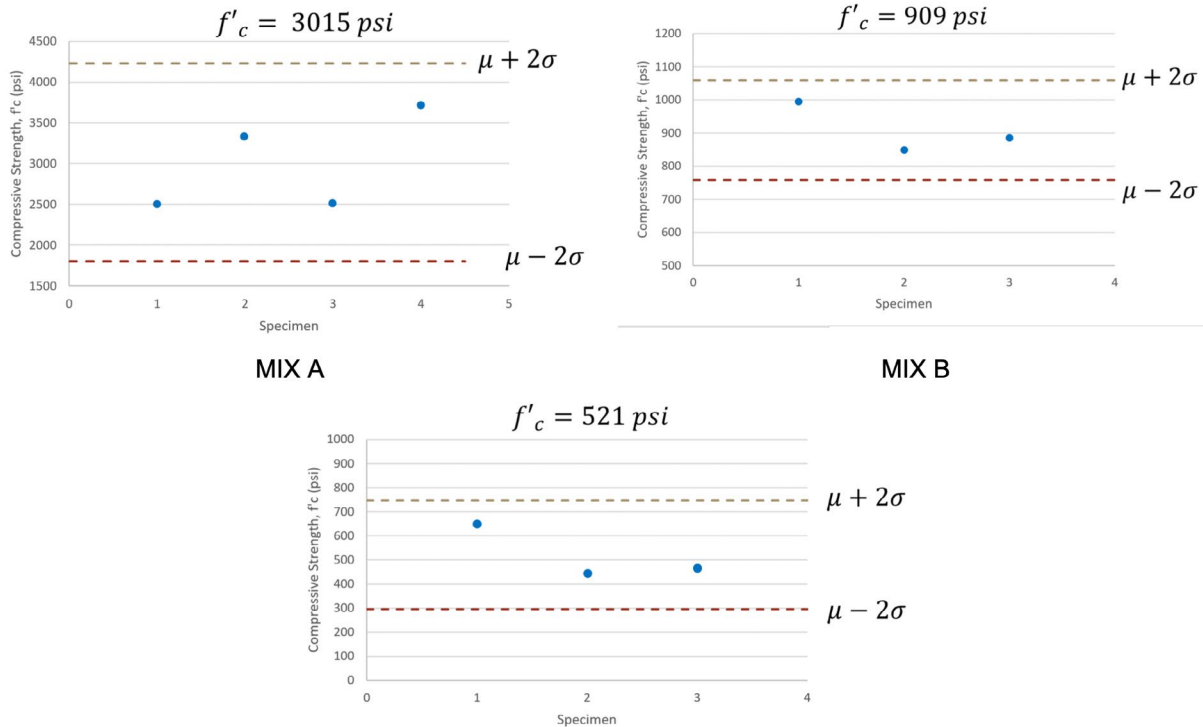
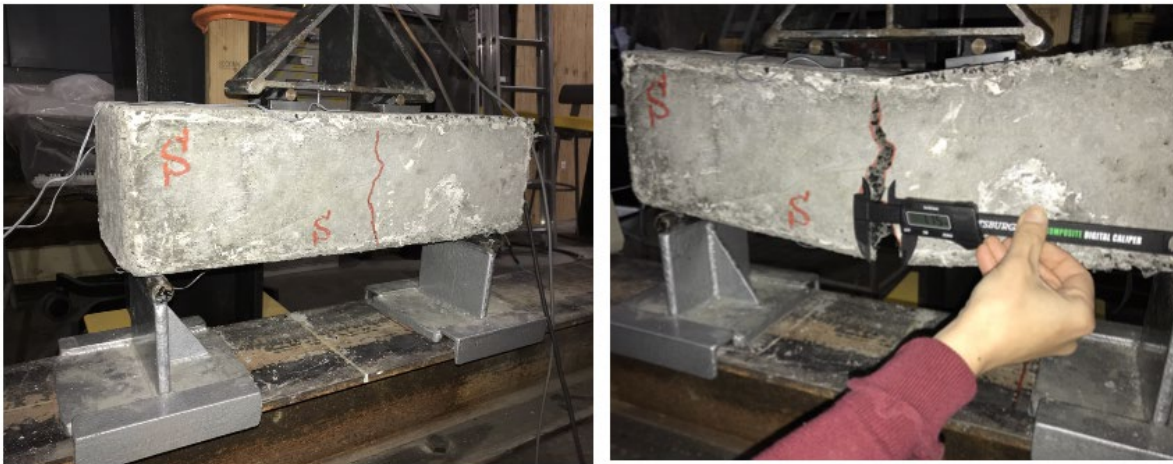


**Figure 13. Average Compressive Strength of Concrete Cylinders (in this figure,  $\mu$  is the average and  $\sigma$  is the standard deviation)**

## PHASE II: PART 1 – STATIC FLEXURAL TESTS OF BEAMS

As summarized in Table 4, three beams from each mix design were tested. In order to quantify the crack formation on each beam and compare them among one another, the specimens' north and south faces were marked and the load at which each crack's width measurement was taken was recorded. The crack formations of MIX A's beams were not measured during experimentation, given that they were expected to exhibit brittle behavior when experiencing load. Figure 14 shows the initial and final crack formation in one of the beams with 100% TDA. According to this figure, rubberized beams sustained larger deformations before failure. The ductile behavior of these beams under the flexural loading was also confirmed by comparing their fracture surfaces, as presented in Figure 14. Note that a flat fracture surface of the MIX A's beam indicates its brittle performance.



Initial and Final Cracks on the south side of beam with Mix C



Fracture Surface of Beams with MIX A, B, and C

### Figure 14. Experimental Observations – Static Flexural Testing of Beams

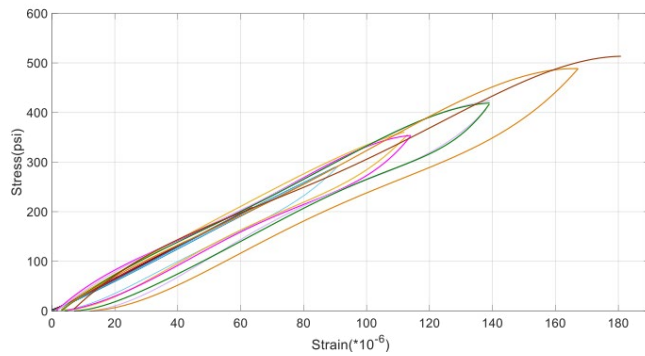
Figure 15 shows the stress-strain curves of the specimens when subjected to multiple cycles of loading up to the point of failure (as depicted by the loading protocol in Figure 7). Due to the space limitations, the responses of three beams with different mix designs (i.e., A, B, and C) are primarily presented here. In the figures included, the tensile stress was calculated from the bending equation, as shown below:

$$\sigma = \frac{Mc}{I} = \frac{\left(\frac{P}{2} \cdot 6\right) \left(\frac{h}{2}\right)}{\frac{bh^3}{12}} = \frac{18P}{bh^2} \quad (3)$$

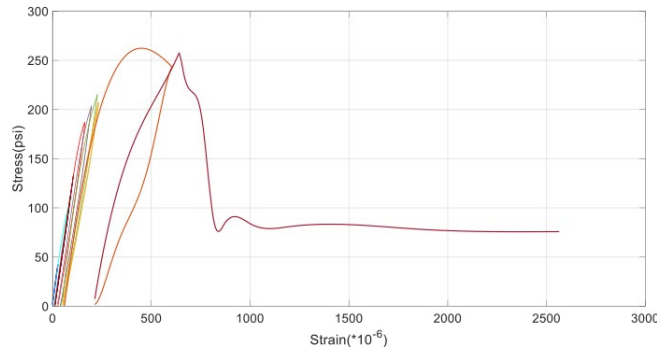
where,  $\sigma$  represents the stress,  $M$  represents the bending moment,  $c$  represents the distance from the neutral axis to the surface of the beam (which was  $0.5h$  given that the beam was of width  $b$  and height  $h$ ),  $I$  represents the moment of inertia (based on the cross-section of the beams), and  $P$  represents the load values. Of these values,  $b$  and  $h$  were measured directly as geometric properties of each beam and  $P$  was recorded using the DataPAC data acquisition system. As shown in the final simplified expression for stress, these three values are the only required measurements needed to compute the

stress values. The ultimate tensile stress, namely the experimental modulus of rupture (MOR), was estimated by using the  $P_{cr}$  in Equation 3. These stress values were then plotted against the strain values, recorded from the strain gauges at the bottom surface of the beam, to yield the following stress–strain curves.

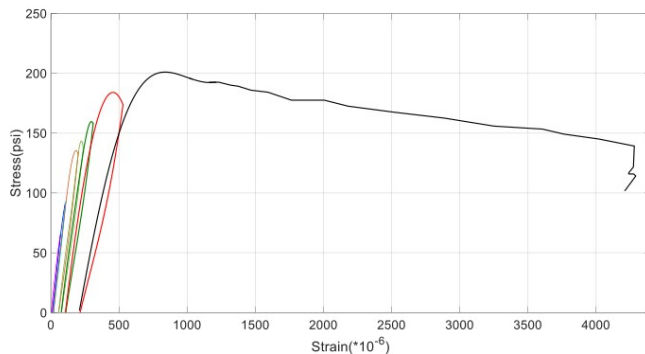
Figure 15 also depicts the comparison of stress-strain plots for the three beams at the final loading cycle, prior to failure. As shown in this figure, adding TDA to the concrete mix resulted in a smaller modulus of rupture but an increased ductility capacity. It should be noted that the stiffness (i.e., the initial slope of the stress-strain curve) of the rubberized beams was reduced after several cycles of loading (i.e., stiffness degradation), which is also depicted in Figure 15.



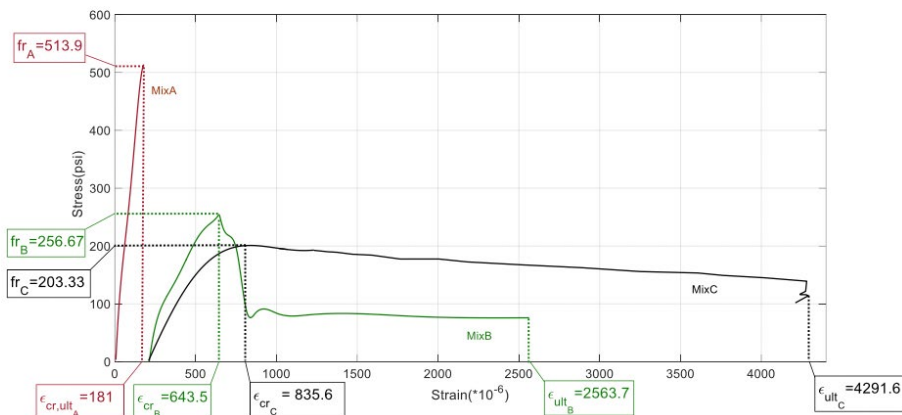
MIX A



MIX B



MIX C



Comparison of plots for different mixes – Final cycle

**Figure 15. Stress-Strain Curves for Beams with MIX A, B, and C**

Table 8 summarizes the critical load, modulus of rupture, stiffness degradation ratio, maximum deflection (using the SPOT readings), and maximum gap opening (measured throughout the test) for beams with MIX A, B, and C.

**Table 8. Summary of Experimental Results – Beams**

Mix design*	Maximum load (lb)	MOR (psi) experiment/ expected**	Stiffness degradation ratio %	Maximum deflection (in.)	Maximum gap opening (in.)
MIX A	6610	514/ 309	4.9	0.08	Sudden failure
MIX B	3160	258/ 170	29.9	0.71	1.29
MIX C	2440	203/ 128	49.3	0.78	1.51

\*only results from one set of beams are presented.

\*\* ACI 318-14,  $f_r = 7.5\lambda\sqrt{f'_c}$ , where  $\lambda=0.75$  for lightweight concrete.

The flexural toughness, or the ability of the specimens to absorb energy before fracture (i.e., energy absorption capacity), depends on both strength and ductility, and it can be estimated as the area under the stress-strain curve. Specimens with higher energy absorption capacity perform satisfactorily when subjected to repeated cycles of loading during their service life due to fatigue. Following ASTM C1018-97, toughness index  $I_5$ , the number obtained by dividing the area up to a deflection of 3.0 times the first-crack, and toughness index  $I_{10}$ , the number obtained by dividing the area up to a deflection of 5.5 times the first-crack deflection by the area up to first crack, were estimated for three beams and plotted in Figure 16. As shown in this figure, the energy absorption capacity of the beams was significantly enhanced by replacing EC with TDA.

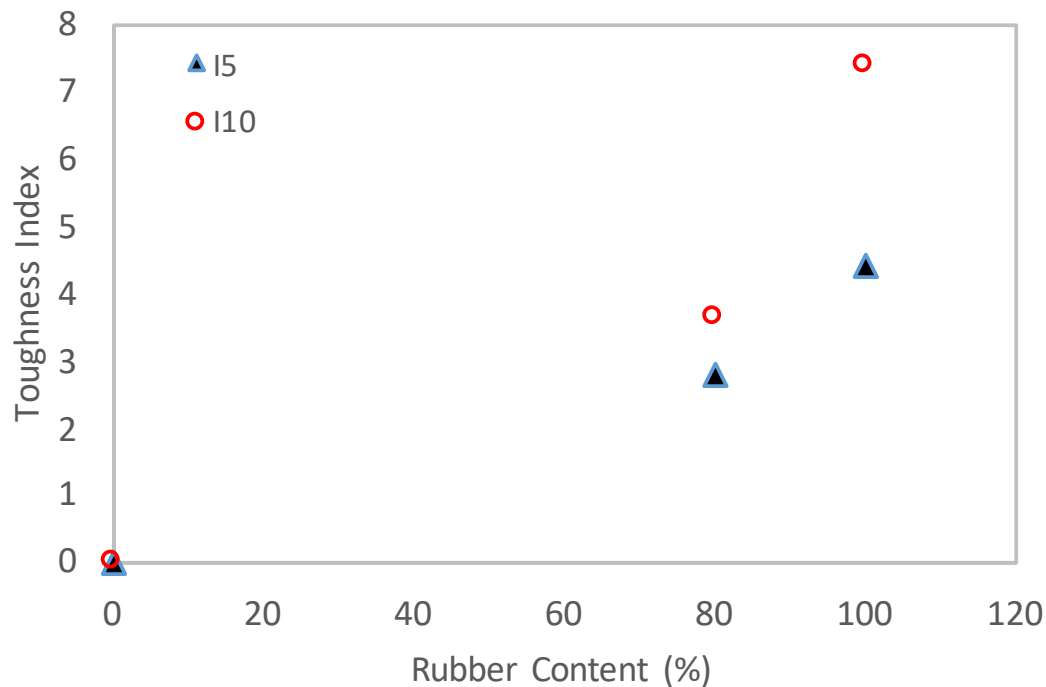
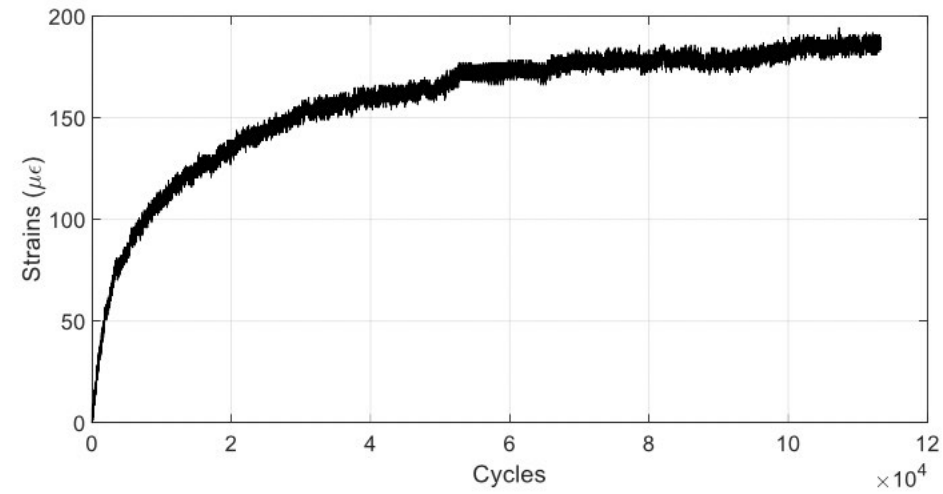


**Figure 16. Flexural Toughness vs Rubber Content in Beams**

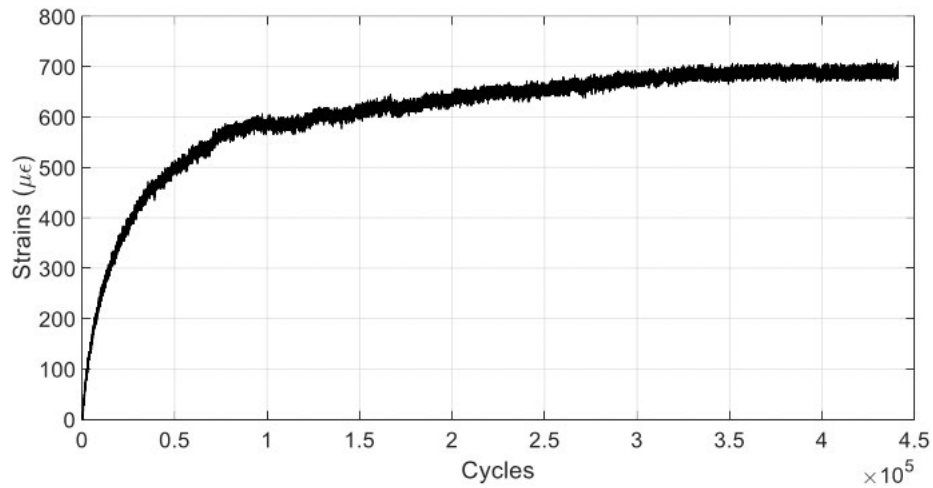
## **PHASE II: PART 2 – IMPACT FATIGUE TESTS OF SLABS**

The slabs were subjected to multiple cycles of impact loading and the testing was conducted until the tensile strain at the bottom surface of the slabs reached the cracking strain. This is defined as the strain corresponding to the maximum tensile stress as measured during flexural testing of the beam specimens. As shown in Figure 15, these strain values are equal to 181, 643.5, and 835.6  $\mu\epsilon$ , respectively for MIX A, B, and C.

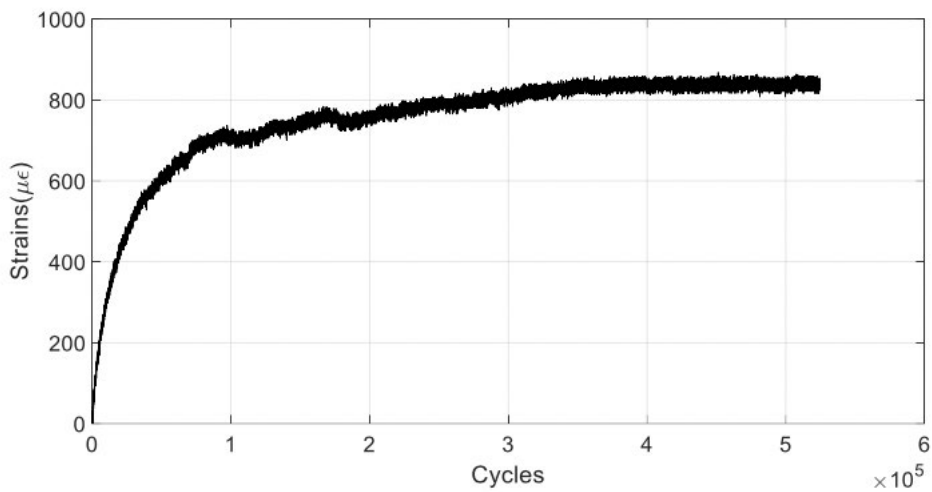
Figure 17 shows the number of loading cycles against the tensile strain measured at the bottom surface of the slabs. As mentioned above, the testing was stopped when the tensile strain reached the cracking values presented in Figure 15.



113252 cycles up to a strain of 181  $\mu\epsilon$  – MIX A



441171 cycles up to a strain of 643.5  $\mu\epsilon$  – MIX B



524590 cycles up to a strain of 835.6  $\mu\epsilon$  – MIX C

**Figure 17. Number of Loading Cycles vs. Strain – Impact Fatigue Testing of Slab Assemblies**

According to the plots depicted in Figure 17, the slab assemblies of MIX A, B, and C experienced 113252, 441171, and 524590 loading cycles up to their ultimate tensile strain, respectively. It can be concluded that replacing 80% and 100% of EC with TDA has increased the durability of slabs by 290% and 363%, respectively. This information was used to perform the life-cycle cost analysis, as presented in the following section.

## V. LIFE-CYCLE COST ANALYSIS

### INITIAL COSTS

The initial cost of concrete involves three proposed mix design proportions in the experimental phase of the project. These mix design proportions include MIX A, B, and C with 100-0, 20-80, and 0-100 volumetric portions of expanded clay and tire-derived aggregates, respectively. Figure 18 presents these values per cubic meter of concrete. Incorporated costs per unit weight of materials utilize actual purchase prices in this project. The cost of placement is essentially identical for all mix designs and hence, does not influence the comparative scope of this study. For comparison purposes, the total cost of construction of a bike lane using conventional concrete, including earthwork and drainage<sup>25</sup>, is nearly 115 \$/m<sup>2</sup>, with the concrete slab cost<sup>26</sup> of nearly 26 \$/m<sup>2</sup>. These yields to nearly 890 \$/m<sup>3</sup> cost of construction excluding the pavement. Thus, the cost of materials for TDA and EC concrete is nearly 30% of the total cost.

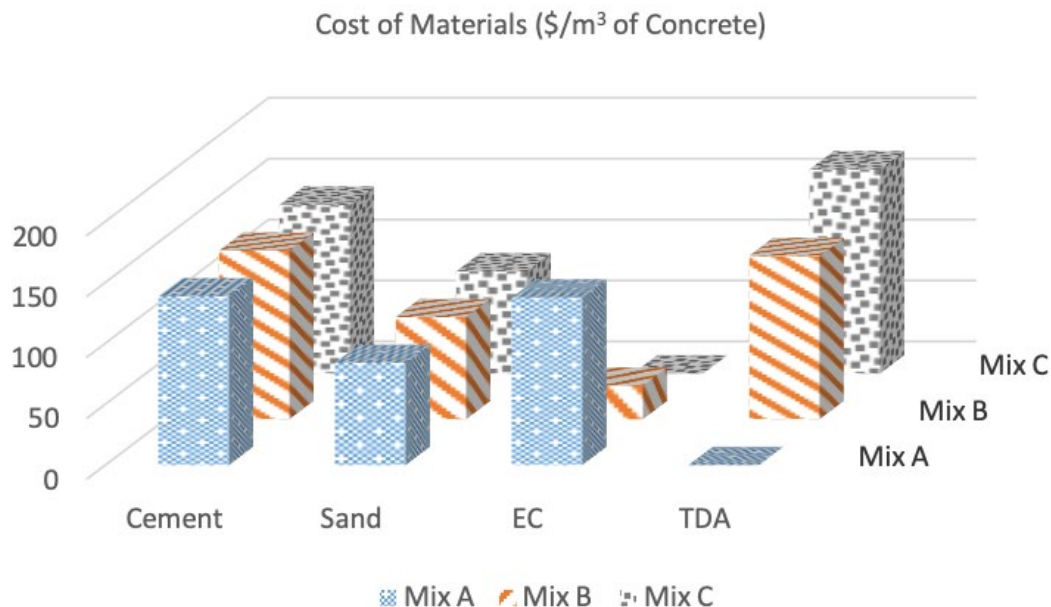


**Figure 18. Initial Cost of Materials Per Cubic Meter of Concrete**

### MAINTENANCE COSTS

Maintenance operations typically include minor preventive maintenance projects to keep the serviceability level of the pavement and major corrective projects to rehabilitate the pavement. Diamond grinding (3.6 \$/m<sup>2</sup>) and patching (120 \$/m<sup>2</sup>) are common practices for these maintenance strategies, where patching is typically needed on 1% of the pavement area only.<sup>26</sup> Thus, the cost of maintenance is effectively 4.8 \$/m<sup>2</sup>. Experimental results in this project, presented in Section IV of the report, have indicated the number of load cycles that are required to reach cracking and failure thresholds. Table 9 lists a summary of these findings. The values of strain at peak and failure were presented in Figure 15. The ductility

ratio in this table is indicative of the ability of pavement to withstand considerable number of traffic load cycles after passing the peak load. Figure 19 provides a schematic view of the relationship between strength and load cycles.

**Table 9. Summary of Experimental Results**

Pavement performance	Peak stress (MPa)	Number of cycles at peak stress	Strain at peak ( $10^{-6}$ mm/mm)	Strain at failure ( $10^{-6}$ mm/mm)	Ductility ratio
Mix A	3.54	113,252	181	181	1
Mix B	1.77	441,171	644	2564	3.98
Mix C	1.40	524,590	836	4292	5.14

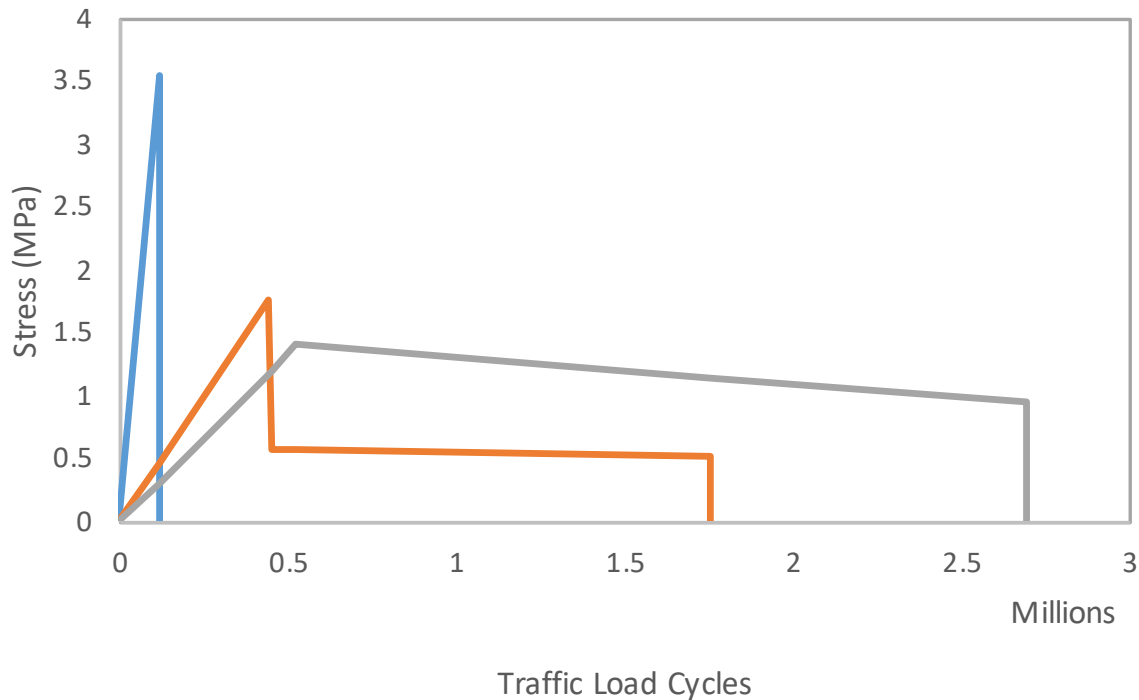


**Figure 19. Schematic Relationship Between Stress and Load Cycles**

Minor maintenance strategies can enhance the serviceability of pavement between peak and failure loads. Replacement is required when the pavement reaches the failure point. The number of cycles may represent time after conversion using the annual average daily traffic of bikes, i.e., 200 AADT for 365 days per year.<sup>27</sup> It is also evident that MIX A has considerably higher peak strength values and thus serves as a more economic design due to its greater optimized sections. Thus, the comparative cost of materials for MIX B and MIX C has been considered based on 140% and 160% of the thickness of MIX A, respectively. Table 10 shows the initial and maintenance costs for a zero-interest economic environment. The results of this table indicate considerable reduction in the life cycle cost due to residual strength of ductile mixtures.

**Table 10. Summary of Cost Analyses**

<b>Life-Cycle Costs</b>	<b>Material Costs<sup>1</sup> (\$/m<sup>3</sup>)</b>	<b>Placement Costs<sup>2</sup> (\$/m<sup>3</sup>)</b>	<b>Maintenance Intervals<sup>3</sup> (year)</b>	<b>Maintenance Costs<sup>4</sup> (\$/m<sup>3</sup>)</b>	<b>Life<sup>3,5</sup> (year)</b>	<b>Annual Value<sup>6</sup> (\$/m<sup>3</sup>)</b>
Mix A	360	890	1.6	48	1.6	811
Mix B	543	890	6.0	48	24	67.7
Mix C	620	890	7.2	48	37	47.5

<sup>1</sup> Adjusted for peak strength

<sup>2</sup> Includes earthwork, drainage, etc.

<sup>3</sup> Assuming AADT = 200

<sup>4</sup> Pavement only, including 100% grinding and 1% patching

<sup>5</sup> Maintenance intervals multiplied by ductility ratios, as summarized in Table 9

<sup>6</sup> Assuming zero interest for simplicity

---

## VI. CONCLUSIONS AND FUTURE RESEARCH

This report presented the results obtained from a series of materials and structural components tests (i.e., compression, static flexural, and dynamic impact-fatigue), as well as life-cycle cost analyses on lightweight rubberized concrete specimens using a total of nine cylinders, nine simply supported beams, and three slab assemblies. Three mix designs were incorporated in this study with 0% (i.e., MIX A or the control mix), 80% (i.e., MIX B), and 100% (i.e., MIX C) Tire-Derived Aggregates (TDA) replacements by the volume of the light-weight Expanded Clay (EC) coarse aggregates. The conclusions drawn from this study are presented below:

- 1. Materials/Compression Testing of Cylinders:* The compressive strength of concrete cylinders was reduced by 70% and 83% by replacing 80% (MIX B) and 100% (MIX C) of EC coarse aggregates with TDA, respectively. It is worth mentioning that the achieved strength was still sufficient in sustaining bicycle loads in non-auto transportation routes. Localized cracks were observed at corners of the rubberized concrete cylinders while one single crack split the control specimen into two pieces. This confirmed a ductile type of fracture in the concrete cylinders with added rubber aggregates compared to the control specimen, which fractured in a brittle manner with little warning prior to complete failure.
- 2. Static Flexural Testing of Beams:* The modulus of rupture (MOR) of the concrete beams was reduced by 50% and 61% by replacing 80% (MIX B) and 100% (MIX C) of EC coarse aggregates with TDA, respectively. On the other hand, the rubberized specimens (i.e., MIX B and C) sustained larger deformations at their mid-spans before their flexural failure. Test results also showed a maximum gap opening of 1.29 and 1.51-inch before failure, respectively for the ductile beams with MIX B and C, while the control beam (MIX A) experienced a sudden failure. Additionally, the flexural toughness was increased by a factor of 2.78 and 4.42 at rubber replacement ratios of 80% and 100%, respectively. This confirmed the higher energy absorption capacity of rubberized concrete specimens.
- 3. Dynamic Impact-Fatigue Testing of Slabs:* By replacing 80% and 100% of EC with TDA, the slab assemblies respectively sustained 2.9 and 3.6 times more cycles of impact loading up to their fatigue failure, compared to the control specimen.
- 4. Life-Cycle Cost Analysis:* Allowing for similar placement and maintenance costs for the three slab assemblies and an AADT of 200, it was concluded that their service life (to reach failure) has been increased from 1.6 years for the control slab to 24 and 37 years for the rubberized slabs with MIX B and C, respectively. The results of this section indicated considerable reduction in the life cycle cost due to residual strength of ductile mixtures.

In conclusion, the application of green strategies for the design and construction of non-auto transportation infrastructure can help improve transportation safety and secure long-term economic benefits of transportation investments. By promoting the use of TDA in non-auto roads/bridge, the diversion of waste tires, which is currently about 40 million per year in California (CalRecycle), from landfills can be increased.

Within the outcomes presented in this report, several additional areas were identified, which require further investigation. A few recommendations for future study include:

1. Enhancing the compressive and flexural strength of rubberized concrete slabs.
2. Considering the impact of different processing methods of TDA on the mechanical properties of rubberized concrete slabs.
3. Studying the effects of existing environmental changes (e.g., temperature changes) on the strength and durability capacities of rubberized concrete slabs.
4. Conducting experimental studies on large-scale prototypes exposed to naturally occurred loads. Such extension may include placement of a concrete slab as part of an existing sidewalk or bike way and measure applied forces and deformations over time.

---

## ABBREVIATIONS AND ACRONYMS

---

AASHTO	American Association of State Highway and Transportation Officials
ASTM	American Society for Testing and Materials
CA	Coarse Aggregate
EC	Expanded Clay
FA	Fine Aggregate
LVDT	Linear Variable Differential Transformer
MOR	Modulus of Rupture
SPOT	String Potentiometer
TDA	Tire Derived Aggregate
UTM	Universal Testing Machine

---

---

## ENDNOTES

1. I. B. Topçu and N. Avcular, "Collision behaviours of rubberized concrete." *Cement and Concrete Research* 27 (12):1893–1898. 1997.
2. M. Al-Tayeb, B. Abu Bakar, H. Akil, and H. Ismail. "Performance of rubberized and hybrid rubberized concrete structures under static and impact load conditions." *Experimental Mechanics* 53 (3):377–384. 2013.
3. F. M. Tehrani, and N. M. Miller, "Tire-derived Aggregate Cementitious Materials: A Review of Mechanical Properties, in Cement-based Materials", Ed. by H. Saleh. Intech. ISBN 978-953-51-5996-4. [dx.doi.org/10.5772/intechopen.74313]. 2018.
4. Ali O. Atahan and Umur K. Sevim., "Testing and comparison of concrete barriers containing shredded waste tire chips." *Materials Letters* 62 (21–22):3754–3757. 2008.
5. Neil N. Eldin, and Ahmed B. Senouci. "Rubber-tire particles as concrete aggregate." *Journal of materials in civil engineering* 5 (4):478–496. 1993.
6. Z. K. Khatib, and F. M. Bayomy. "Rubberized Portland cement concrete." *Journal of materials in civil engineering* 11 (3):206–213. 1999
7. I. B. Topçu. "The properties of rubberized concretes." *Cement and concrete research* 25 (2):304–310. 1995.
8. K. E. Kaloush, G. B. Way, and Han Zhu. "Properties of crumb rubber concrete." *Transportation Research Record: Journal of the Transportation Research Board* (1914):8–14. 2005.
9. H. Rostami, J. Lepore, T. Silverstraim, and I. Zundi. "Use of recycled rubber tires in concrete." In *Proceedings of the international conference on concrete*, vol. 1993, pp. 391–399. London, United Kingdom: Thomas Telford Services Ltd. 2000.
10. N. Segre, and I. Joeke. "Use of tire rubber particles as addition to cement paste." *Cement and concrete research* 30 (9):1421–1425. 2000.
11. Rafat Siddique, and Tarun R. Naik. "Properties of concrete containing scrap-tire rubber—an overview." *Waste management* 24 (6):563–569. 2004.
12. ASTM C78. "Standard test method for flexural strength of concrete (using simple beam with third-point loading)." 2010.
13. T.S. Vadivel, R. Thenmozhi, and M. Doddurani. "Experimental behaviour of waste tyre rubber aggregate concrete under impact loading". *Iranian Journal of Science and Technology - Transactions of Civil Engineering*. (38): 251-259. 2014.

14. N. M. Miller, and F. M. Tehrani. "Mechanical properties of rubberized lightweight aggregate concrete." *Construction and Building Materials* 147(30):264–271. 2017.
15. How-Ji Chen, Chung-Ho Huang, and Chao-Wei Tang. "Dynamic Properties of Lightweight Concrete Beams Made by Sedimentary Lightweight Aggregate." *Journal of Materials in Civil Engineering* 22 (6):599–606. doi: 10.1061/(ASCE)MT.1943-5533.0000061. 2010.
16. Satish Chandra, and Leif Berntsson. "Lightweight aggregate concrete". Elsevier. ISBN: 9780815518204. 2002.
17. T.A. Holm, and A.J. Valsangkar. "Lightweight aggregate soil mechanics: properties and applications." *Transportation research record* 1422:7. 1993.
18. ACI Committee 318. "Building Code Requirements for Structural Concrete (ACI 318–14) and Commentary (ACI 318R–14)." American Concrete Institute, Farmington Hills, MI:519. 2014.
19. Seung Woo Lee, Yoon-Ho Cho, and Cheolwoo Park. "Mechanical performance and field application of low cement-based concrete under compaction energy." *KSCE Journal of Civil Engineering* 18 (4):1053–1062. 2014.
20. ASTM C39/C39M. "Standard Test Method for Compressive Strength of Cylindrical Concrete Specimens. *ASTM International*, West Conshohocken. 2016.
21. P. Manghera, F. Rahman, S. Banerjee, and M. Nazari. "Application of electro-active materials toward health monitoring of structures: electrical properties of smart aggregates", Proceedings of IMAC XXXVII – Society for Experimental Mechanics (SEM) Conference, Orlando, Florida. 2019.
22. ACI Committee 437. "Test load magnitude, protocol and acceptance criteria." ACI 437.1R-07, ACI Committee 437, Farmington Hills, Mich. 2007.
23. CSI. "SAP2000 v14 Integrated Finite Element Analysis and Design of Structures". CSI, Berkeley, CA. 2013.
24. FEMA-356. "Prestandard and Commentary for Seismic Rehabilitation of Buildings", Washington DC. 2000.
25. M.A. Bushell, Bryan W. Poole, Charles V. Zegeer, and Daniel A. Rodriguez. "Costs for Pedestrian and Bicyclist Infrastructure Improvements". A Resource for Researchers, Engineers, Planners, and the General Public, UNC Highway Safety Research Center. 2013.
26. P. Vosoughi, S. Tritsch, H. Ceylan, and P. C. Taylor. "Lifecycle Cost Analysis of Internally Cured Jointed Plain Concrete Pavement". *InTrans Project Reports*. 222. 2017.

27. Tianjun Lu. "Bicycle and Pedestrian Traffic Monitoring and AADT Estimation in a Small Rural College Town". Master's Thesis, Virginia Polytechnic Institute and State University. 2016.

---

## BIBLIOGRAPHY

- ACI Committee 213. "Guide to Structural Lightweight Aggregate Concrete (ACI 213–R14)." American Concrete Institute, Farmington Hills, MI, 2014.
- ACI Committee 318. "Building Code Requirements for Structural Concrete (ACI 318–14) and Commentary (ACI 318R–14)." American Concrete Institute, Farmington Hills, MI:519, 2014.
- Al-Tayeb, MM, BH Abu Bakar, HM Akil, and H Ismail. "Performance of rubberized and hybrid rubberized concrete structures under static and impact load conditions." *Experimental Mechanics* 53, no. 3 (2013):377–384.
- ASTM C39/C39M. "Standard Test Method for Compressive Strength of Cylindrical Concrete Specimens. *ASTM International*, West Conshohocken, 2016.
- ASTM C78. "Standard test method for flexural strength of concrete (using simple beam with third-point loading)." ASTM International, West Conshohocken, PA, 2010.
- ACI Committee 437. "Test load magnitude, protocol and acceptance criteria." ACI 437.1R-07, ACI Committee 437, Farmington Hills, Mich, 2007.
- Atahan, Ali O, and Umur K Sevim. "Testing and comparison of concrete barriers containing shredded waste tire chips." *Materials Letters* 62, no. 21–22 (2008):3754–3757.
- Bushell M.A., Bryan W. Poole, Charles V. Zegeer, and Daniel A. Rodriguez. "Costs for Pedestrian and Bicyclist Infrastructure Improvements". A Resource for Researchers, Engineers, Planners, and the General Public, UNC Highway Safety Research Center, 2013.
- California Integrated Waste Management Board. "Effects of Waste Tires, Waste Tire Facilities, and Waste Tire Projects on the Environment." May 1996, calrecycle.ca.gov.
- Chandra, Satish, and Leif Berntsson. "Lightweight aggregate concrete". Elsevier (2002). ISBN: 9780815518204.
- Chen, How-Ji, Chung-Ho Huang, and Chao-Wei Tang. "Dynamic Properties of Lightweight Concrete Beams Made by Sedimentary Lightweight Aggregate." *Journal of Materials in Civil Eng.* 22, no. 6 (2010):599–606. doi: 10.1061/(ASCE)MT.1943-5533.0000061.
- CSI (Computers and Structures Inc. "SAP2000 v14 Integrated Finite Element Analysis and Design of Structures". CSI, Berkeley, CA, 2013.

- Eldin, Neil N, and Ahmed B Senouci. "Rubber-tire particles as concrete aggregate." *Journal of materials in civil engineering* 5, no. 4 (1993):478–496.
- Federal Emergency Management Agency, FEMA-356. "Prestandard and Commentary for Seismic Rehabilitation of Buildings", Washington DC, 2000.
- Holm, TA, and AJ Valsangkar. "Lightweight aggregate soil mechanics: properties and applications." *Transportation research record* (1993) 1422:7.
- Kaloush, Kamil, George Way, and Han Zhu. "Properties of crumb rubber concrete." *Transportation Research Record: Journal of the Transportation Research Board* 2005. 8-14. 10.3141/1914-02
- Khatib, Zaher K, and Fouad M Bayomy. "Rubberized Portland cement concrete." *Journal of materials in civil engineering* 11, no. 3 (1999):206–213.
- Lee, Seung Woo, Yoon-Ho Cho, and Cheolwoo Park. "Mechanical performance and field application of low cement-based concrete under compaction energy." *KSCE Journal of Civil Engineering* 18, no. 4 (2014):1053–1062.
- Lu Tianjun. "Bicycle and Pedestrian Traffic Monitoring and AADT Estimation in a Small Rural College Town". Master's Thesis, Virginia Polytechnic Institute and State University, 2016.
- Manghera, Patrick, Faiaz Rahman, Sankha Banerjee, and Maryam Nazari. "Application of electro-active materials toward health monitoring of structures: electrical properties of smart aggregates", Proceedings of IMAC XXXVII – Society for Experimental Mechanics (SEM) Conference, Orlando, Florida, 2019.
- Miller, Nathan M, and Fariborz M Tehrani. "Mechanical properties of rubberized lightweight aggregate concrete." *Construction and Building Materials* 147, no. 30 (2017):264–271.
- Rostami, H., J. Lepore, T. Silverstraim, and I. Zundi. "Use of recycled rubber tires in concrete." In *Proceedings of the international conference on concrete*, vol. 1993, pp. 391–399. London, United Kingdom: Thomas Telford Services Ltd. 2000.
- Segre, N, and I. Joekes. "Use of tire rubber particles as addition to cement paste." *Cement and concrete research* 30, no. 9 (2000):1421–1425.
- Siddique, Rafat, and Tarun R. Naik. "Properties of concrete containing scrap-tire rubber—an overview." *Waste management* 24, no. 6 (2004):563–569.
- Tehrani, F. M., and N. M. Miller. "Tire-derived Aggregate Cementitious Materials: A Review of Mechanical Properties, in Cement-based Materials", Ed. by H. Saleh. Intech. ISBN 978-953-51-5996-4. [dx.doi.org/10.5772/intechopen.74313], 2018.

- Topçu, I. B., and N. Avcular. "Collision behaviours of rubberized concrete." *Cement and Concrete Research* 27, no. 12 (1997):1893–1898.
- Topcu, Ilker Bekir. "The properties of rubberized concretes." *Cement and concrete research* 25, no. 2 (1995):304–310.
- Vadivel, Senthil, R. Thenmozhi, and M. Doddurani. "Experimental behaviour of waste tyre rubber aggregate concrete under impact loading". *Iranian Journal of Science and Technology - Transactions of Civil Engineering*. no. 38 (2014): 251-259.
- Vosoughi, Payam, Steven Tritsch, Halil Ceylan, and Peter C. Taylor. "Lifecycle Cost Analysis of Internally Cured Jointed Plain Concrete Pavement". *InTrans Project Reports*. 222 (2017).

---

## ABOUT THE AUTHORS

### MARYAM NAZARI

Dr. Maryam Nazari is an Assistant Professor of Structural Engineering in the Department of Civil and Geomatics Engineering at CSU, Fresno. Her research interest is the application of seismic-resilient precast concrete solutions for design of structures. During her graduate studies, she worked on a research study funded by the National Science Foundation (NSF). She accomplished large-scale shake table experiments on self-centering precast concrete wall systems at the Network for Earthquake Engineering Simulation (NEES) facility of the University of Nevada at Reno (UNR), with the purpose of investigating the impact of different energy dissipating components of these innovative structural systems on their seismic responses. She also participated in several rehabilitation and strengthening projects during her five-year professional experience as a structural design engineer, seismic specialist, and project manager. She has about 10 peer-reviewed conference proceedings and journal papers and has done more than 10 presentations in national and international conferences as well as technical meetings. Her recent research awards include the ASCE Fresno Best Research Project (in collaborations with Dr. Tehrani), SEI/ASCE Young Professional Scholarship, and the Iowa State University's Research Excellence award.

### FARIBORZ TEHRANI

Dr. Fariborz Tehrani is an Associate Professor of Civil Engineering at California State University, Fresno, with research and practice background in Sustainable and Resilient Structural Engineering, Mechanics, and Materials (SR-SEMM). He has practiced transportation engineering in the California Department of Transportation and has performed multiple research projects in the areas of lightweight aggregates and concrete materials, and has received external funding for research projects from the California Department of Transportation, National Science Foundation, and other professional entities. His extensive background and credentials in engineering design (PE), management (PMP), and sustainable practices (ENV SP) have enabled him to integrate research with education and practice, which has been the key in his teaching success. Over the past seven years, he has established a diverse research and practice group to attract underrepresented students and has mentored numerous students on their thesis and projects. He is the recipient of multiple awards, including ASCE CA Outstanding Faculty, CHESC Best Practice, and ASCE Fresno Best Research Project.

### MOJTABA ANSARI

Mojtaba Ansari is a visiting scholar and Ph.D. student at Fresno State. He received his bachelor's and master's degrees, respectively, from Shiraz University and Sharif University of Technology, Iran, in Civil/Earthquake Engineering and is currently a Ph.D. student at Tarbiat Modares University, Iran. His main research interests include seismic soil-structure interaction, seismic hazard analysis, numerical and physical modeling of soil-structure systems, and seismic risk assessment of structures. His doctoral research

works towards shake table testing of structures sitting on pile foundations to assess the seismic vulnerability of the superstructure.

### **BHAVESH JEEVANLAL**

Bhavesh Jeevanlal received his master's degree in Civil Engineering at Fresno State. He has co-authored a conference paper, and was also a Dean's Medalist Nominee during his master's program. He is actively working with a precast firm in California as a project engineer. He is also an active member of ASCE and ACI.

### **FAIAZ RAHMAN**

Faiaz Rahman is an undergraduate student studying electrical engineering and computer science. As a former civil engineering student at the time of this study, Faiaz explored the sustainable development of infrastructure and its applications in urban systems. A native of Bangladesh interested in the intersection of education and technology along with intelligent urban systems, Faiaz hopes to expand the accessibility of educational resources to underserved and underdeveloped parts of the world, where advancements in sustainable infrastructure will further aid in their development.

### **ROSHANAK FARSHIDPOUR**

Roshanak Farshidpour is currently an undergraduate student pursuing a Civil Engineering degree at CSU Fresno. She will be obtaining a bachelor's degree with an emphasis in Structural Engineering in the Spring of 2019. Roshanak hopes to pursue a master's in Structural and Earthquake Engineering in Fall 2019 at UCLA. Ultimately, she aims to work towards creating projects that will direct the field of Civil Engineering towards innovative, sustainable, and economic approaches.

## MTI BOARD OF TRUSTEES

**Founder, Honorable Norman Mineta (Ex-Officio)**  
Secretary (ret.),  
US Department of Transportation

**Chair, Grace Crunican (TE 2019)**  
General Manager  
Bay Area Rapid Transit District (BART)

**Vice Chair, Abbas Mohaddes (TE 2021)**  
President & COO  
Econolite Group Inc.

**Executive Director, Karen Philbrick, Ph.D. (Ex-Officio)**  
Mineta Transportation Institute  
San José State University

**Richard Anderson (Ex-Officio)**  
President & CEO  
Amtrak

**Laurie Berman (Ex-Officio)**  
Director  
California Department of Transportation (Caltrans)

**David Castagnetti (TE 2021)**  
Co-Founder  
Mehlman Castagnetti  
Rosen & Thomas

**Maria Cino (TE 2021)**  
Vice President  
America & U.S. Government  
Relations Hewlett-Packard Enterprise

**Donna DeMartino (TE 2021)**  
General Manager & CEO  
San Joaquin Regional Transit District

**Nuria Fernandez\* (TE 2020)**  
General Manager & CEO  
Santa Clara Valley  
Transportation Authority (VTA)

**John Flaherty (TE 2020)**  
Senior Fellow  
Silicon Valley American  
Leadership Form

**Rose Guilbault (TE 2020)**  
Board Member  
Peninsula Corridor  
Joint Powers Board

**Ian Jefferies (Ex-Officio)**  
President & CEO  
Association of American Railroads

**Diane Woodend Jones (TE 2019)**  
Principal & Chair of Board  
Lea + Elliott, Inc.

**Will Kempton (TE 2019)**  
Retired

**Jean-Pierre Loubinoux (Ex-Officio)**  
Director General  
International Union of Railways (UIC)

**Bradley Mims (TE 2020)**  
President & CEO  
Conference of Minority  
Transportation Officials (COMTO)

**Jeff Morales (TE 2019)**  
Managing Principal  
InfraStrategies, LLC

**Dan Moshavi, Ph.D. (Ex-Officio)**  
Dean, Lucas College and  
Graduate School of Business  
San José State University

**Takayoshi Oshima (TE 2021)**  
Chairman & CEO  
Allied Telesis, Inc.

**Paul Skoutelas (Ex-Officio)**  
President & CEO  
American Public Transportation  
Association (APTA)

**Dan Smith (TE 2020)**  
President  
Capstone Financial Group, Inc.

**Beverly Swaim-Staley (TE 2019)**  
President  
Union Station Redevelopment  
Corporation

**Larry Willis (Ex-Officio)**  
President  
Transportation Trades  
Dept., AFL-CIO

**Jim Thymon (Ex-Officio)**  
Executive Director  
American Association of  
State Highway and Transportation  
Officials (AASHTO)  
[Retiring 12/31/2018]

(TE) = Term Expiration  
\* = Past Chair, Board of Trustees

## Directors

**Karen Philbrick, Ph.D.**  
Executive Director

**Hilary Nixon, Ph.D.**  
Deputy Executive Director

**Asha Weinstein Agrawal, Ph.D.**  
Education Director  
National Transportation Finance  
Center Director

**Brian Michael Jenkins**  
National Transportation Security  
Center Director

## Research Associates Policy Oversight Committee

**Jan Botha, Ph.D.**  
Civil & Environmental Engineering  
San José State University

**Katherine Kao Cushing, Ph.D.**  
Environmental Science  
San José State University

**Dave Czerwinski, Ph.D.**  
Marketing and Decision Science  
San José State University

**Frances Edwards, Ph.D.**  
Political Science  
San José State University

**Taeho Park, Ph.D.**  
Organization and Management  
San José State University

**Christa Bailey**  
Martin Luther King, Jr. Library  
San José State University

